

The fate of river organic carbon in coastal areas: A study in the Rhône River delta using multiple isotopic ($\delta^{13}\text{C}$, $\Delta^{14}\text{C}$) and organic tracers

C. Cathalot^{a,*}, C. Rabouille^a, N. Tisnérat-Laborde^a, F. Toussaint^a, P. Kerhervé^{b,c}, R. Buscail^{b,c}, K. Loftis^d, M.-Y. Sun^d, J. Tronczynski^e, S. Azoury^e, B. Lansard^a, C. Treignier^a, L. Pastor^f, T. Tesi^{g,h}

^a Laboratoire des Sciences du Climat et de l'Environnement, CEA/CNRS/UVSQ, Gif-sur-Yvette, France

^b CNRS, Centre de Formation et de Recherche sur les Environnements Méditerranéens, UMR 5110, F-66860 Perpignan, France

^c Univ. Perpignan Via Domitia, Centre de Formation et de Recherche sur les Environnements Méditerranéens, UMR 5110, F-66860 Perpignan, France

^d Department of Marine Sciences, University of Georgia, Athens, GA 30602, USA

^e Laboratoire Biogéochimie des Contaminants Organiques, IFREMER, Nantes, France

^f Laboratoire de Géochimie des Eaux, Université Paris VII, Paris, France

^g ISMAR-CNR UOS di Bologna Istituto di Scienze Marine, P. Gobetti, 101 40129 Bologna, Italy

^h Institute of Applied Environmental Research (ITM), Stockholm University, 106 91 Stockholm, Sweden

*: Corresponding author : Cécile Cathalot, tel.: +33 (0) 2 98 22 47 54 ; fax: +33 (0) 2 98 22 47 57 ; email addresses : Cecile.Cathalot@ifremer.fr ; Cecile.Cathalot@nioz.nl

Abstract:

A significant fraction of the global carbon flux to the ocean occurs in River-dominated Ocean Margins (RiOMar) although large uncertainties remain in the cycle of organic matter (OM) in these systems. In particular, the OM sources and residence time have not been well clarified. Surface (0–1 cm) and sub-surface (3–4 cm) sediments and water column particles (bottom and intermediate depth) from the Rhône River delta system were collected in June 2005 and in April 2007 for a multi-proxy study. Lignin phenols, black carbon (BC), proto-kerogen/BC mixture, polycyclic aromatic hydrocarbons (PAHs), carbon stable isotope ($\delta^{13}\text{C}_{\text{OC}}$), and radiocarbon measurements ($\Delta^{14}\text{C}_{\text{OC}}$) were carried out to characterize the source of sedimentary organic material and to address degradation and transport processes. The bulk OM in the prodelta sediment appears to have a predominantly modern terrigenous origin with a significant contribution of modern vascular C_3 plant detritus ($\Delta^{14}\text{C}_{\text{OC}} = 27.9\text{‰}$, $\delta^{13}\text{C}_{\text{OC}} = -27.4\text{‰}$). In contrast, the adjacent continental shelf, below the river plume, seems to be dominated by aged OM ($\Delta^{14}\text{C}_{\text{OC}} = -400\text{‰}$, $\delta^{13}\text{C}_{\text{OC}} = -24.2\text{‰}$), and shows no evidence of dilution and/or replacement by freshly produced marine carbon. Our data suggest an important contribution of black carbon (50% of OC) in the continental shelf sediments. Selective degradation processes occur along the main dispersal sediment system, promoting the loss of a modern terrestrial OM but also proto-kerogen-like OM. In addition, we hypothesize that during the transport across the shelf, a long term resuspension/deposition loop induces efficient long term degradation processes able to rework such refractory-like material until the OC is protected by the mineral matrix of particles.

66 1. INTRODUCTION

67 River-dominated Ocean Margins (RiOMar) play a critically-important role in the
68 biogeochemical cycles of carbon, as they receive large amounts of riverine inputs of carbon
69 and nutrients, sustaining large biological activity (Bianchi and Allison, 2009; Dagg et al.,
70 2004; McKee et al., 2004). High rates of organic carbon (OC) burial and mineralization
71 represent substantial sink and source terms in the carbon budget for the coastal ocean,
72 providing insights on the underlying processes (Borges, 2005; Hedges, 1992). For instance,
73 OC burial is the second largest atmospheric CO₂ sink and plays a major role in long-term
74 climate regulation (Berner, 1990). Terrestrial OC (OC_{terr}) originating from both continental
75 erosion and river autochthonous production can be selectively degraded, deposited and buried
76 in continental margins. The fraction of organic matter that escape either mineralization or
77 burial in the shelf is then exported to the open ocean. OC burial efficiency in RiOMar areas is
78 directly linked to the nature of terrestrial OC delivered to the coastal ocean because different
79 origins and residence time ensure a wide range of reactivity (Hartnett et al., 1998; Hedges and
80 Keil, 1995). Studying the structure, distributions and quantities of terrestrial organic matter, as
81 well as processes governing its fate in the coastal ocean is a key for assessing global
82 biogeochemical cycles (Galy et al., 2007; Raymond and Bauer, 2001a).

83 The Rhône River is the largest river input to the Mediterranean, both in term of water
84 and particulate discharge rates (Ludwig et al., 2003), since the Nile River has been dammed.
85 The Rhône River constitutes 80% of the total riverine inputs into the Gulf of Lions, the
86 Northwestern Mediterranean continental margin, and provides $1.6 \pm 0.5 \times 10^{10}$ mol C y⁻¹ to the
87 Mediterranean Sea (Sempéré et al., 2000). In this context, the export and the fate of this
88 terrestrial material from the Rhône River have been the subject of many intensive physical,
89 biogeochemical and oceanographic studies (Estournel et al., 2001; Radakovitch et al., 1999b;

90 Roussiez et al., 2006; Tesi et al., 2007a; Ulses et al., 2008). These studies used radionuclide-
91 based tracers that provided new insights into particle transfer processes although questions
92 about the fate of river-borne organic matter still need to be addressed. Until recently, studies
93 of particulate organic carbon cycling were mainly focused on off-shelf and canyon transfers
94 rather than continental shelf distribution and margin processes (Tesi et al., 2010b). Thus,
95 although the organic composition of the exported material was fairly well constrained in these
96 studies, little insight is know about the chemical changes along the sediment transport in the
97 shelf. Based on the results from Tesi et al (2007), Lansard et al (2009) made a first
98 quantification of the terrigenous OC fractions of the Rhône River particles using stable
99 carbon isotopes ($\delta^{13}\text{C}$), C/N ratios and lignin-derived biomarkers. Their estimation relies on a
100 two end-member mixing model between terrestrial and marine OC, and it is constrained by a
101 narrow range of $\delta^{13}\text{C}$ values. However, an approach like this can yield only a few information
102 on the reactivity of the sedimentary OC.

103 To better understand the OM cycles in RiOMar systems and provide new insight about
104 residence time and reactivity of sedimentary OC, additional tracers are required to estimate
105 the contribution of terrestrial organic matter to continental margins and its fate. Radiocarbon
106 values ($\Delta^{14}\text{C}$), measured by accelerator mass spectrometry, have proven to be a powerful tool
107 to investigate the dynamics of OC in river systems and marine environments (Druffel et al.,
108 2005; Hedges et al., 1986a; Megens et al., 2001; Raymond and Bauer, 2001b). Radiocarbon
109 can provide useful information on the sources and residence times of particulate organic
110 matter (POM). Organic matter in river suspended particles presents a wide range of $\Delta^{14}\text{C}$
111 signatures from -980 to +75‰ (Blair et al., 2003; Druffel and Williams, 1991; Galy et al.,
112 2007; Hedges et al., 1986b; Nagao et al., 2005; Raymond and Bauer, 2001a) whereas
113 plankton and marine particulate organic carbon (POC) usually display enriched values from -
114 45 to + 110‰ (Wang et al., 1998; Williams et al., 1992). Nevertheless, each river system

115 exhibits a contrasting range of $\Delta^{14}\text{C}$ values of organic matter, reflecting both sediment
116 transport processes within the watershed and local autochthonous production (Goni et al.,
117 2006). This varying range of $\Delta^{14}\text{C}$ values has been applied to distinguish sources of the
118 deposited material (Blair et al., 2003; Goni et al., 1997). Furthermore, the combined use of
119 $\Delta^{14}\text{C}$ and $\delta^{13}\text{C}$ adds a second dimension to assess the carbon cycling in river-dominated
120 margins, especially to determine the fate and reactivity of particulate OC (Drenzek et al.,
121 2007).

122 In this study, we used a multi-proxy approach on both sediments and suspended
123 particles, combining $\Delta^{14}\text{C}$ and $\delta^{13}\text{C}$ of bulk OC, lignin-derived biomarkers and their
124 compound-specific $\delta^{13}\text{C}$, and polycyclic aromatic hydrocarbons (PAHs), black carbon (BC)
125 and proto-kerogen/BC mixture, to elucidate the fate of terrestrial particulate organic matter
126 released from the Rhône River to the Gulf of Lions continental margin. The chemical and
127 isotopic analyses for these samples were modelled based on a four end-members model. The
128 relative contributions of organic matter from various sources were quantitatively examined
129 and the importance of pre-aged OC from continental shelf particles was demonstrated.

130 **2. BACKGROUND**

131 The Rhône River is the major source of freshwater, nutrients and organic carbon to the Gulf
132 of Lions, a large continental shelf located in the NW Mediterranean Sea (De Madron et al.,
133 2000; Pont et al., 2002; Sempéré et al., 2000). The Rhône River flows from the mountain
134 range of the Alps to the Mediterranean Sea, where a delta is formed at its mouth. The
135 catchment area of the Rhône River displays a strong climatic and geological heterogeneity
136 since it drains oceanic, mountainous and Mediterranean weather systems over an area of 97
137 800 km². As an example of the catchment heterogeneity, part of the Durance River's basin
138 (14 000 km²) is very rich in clay, devoid of vegetation and subjected to intense erosion

139 (Richy, 1992) when an important part of the Rhône River watershed consists of carbonate
140 rocks (Pont et al., 2002). A consequence of such heterogeneity is a great variability in the
141 hydrological regime of the Rhône River in terms of precipitation and solid transport capacity,
142 with large differences between low ($<700 \text{ m}^3 \text{ s}^{-1}$) and high ($>3000 \text{ m}^3 \text{ s}^{-1}$) water -discharge
143 rates (Pont et al., 2002). Most of the solid discharge is transported during Mediterranean
144 floods but the mineralogical composition of the suspended matter reaching the river mouth is
145 highly related to the flood origin (Ollivier et al., 2010; Pont et al., 2002). Similarly, the
146 organic material exported at the Rhône River mouth derives from various allochthonous
147 sources (vascular plants, bacteria and soils) and varies with flood events (Panagiotopoulos et
148 al., 2012).

149 Large amount of terrestrial material is deposited in the sediments off the Rhône River mouth
150 between 0 and 20 m water depth (Maillet et al., 2006). In fact, most of the material delivered
151 by the Rhône River accumulates in the prograding prodelta (Fig.1) which extends from the
152 shoreline to 60 m depth with a significant slope (Maillet et al., 2006; Wright and Friedrichs,
153 2006). Net sedimentation rates in the prodelta range from 20 to 50 cm y^{-1} at shallow stations
154 (20 m) near the river mouth (Charmasson et al., 1998; Radakovitch et al., 1999a) down to ≈ 1
155 cm y^{-1} at 60 m water depth where the prodelta ends. The remainder of the Rhône River
156 sediment delivered to the sea is transported and deposited onto the continental shelf at a mean
157 rate $< 0.3 \text{ cm yr}^{-1}$ (Miralles et al., 2005; Radakovitch et al., 1999a; Zuo et al., 1997).

158 The Northwestern Mediterranean current flowing southwestward along the slope imposes a
159 general cyclonic circulation on the continental shelf of the Gulf of Lions (Fig. 1;(Milot,
160 1990). Episodic southeasterly storms may cause the resuspension of Rhône River prodeltaic
161 deposits that are then transported to the southwestern end of the shelf (Roussiez et al., 2005;
162 Ulses et al., 2008). The Gulf of Lions is oligotrophic and the water column is seasonally

163 stratified. Intense vertical mixing events occur in winter and early spring due to strong
164 regional winds and induce major nutrient export, through cascading and dense water
165 formation (de Madron et al., 2003; Millot, 1990).

166 This study investigates the transition zone between the Rhône River prodelta and the Gulf of
167 Lions continental shelf. Most of the changes in sedimentation rates happen within this zone
168 subjected to resuspension (Fig. 1). We expect therefore significant changes in organic matter
169 composition and new insights into the sediment transport system off the Rhône River mouth.

170 **3. MATERIAL AND METHODS**

171 **3.1. Sampling**

172 **3.1.1. River sampling**

173 Suspended particulate matter (SPM) from the Rhône River were sampled monthly from 2006-
174 2009 at the Arles monitoring station (Maillet et al., 2006). The automatic sampler (CALYPSO
175 2000S) is located 50 cm from the surface and 3 m from the bank, and the sampling is assumed
176 to be representative of the entire water column due to the homogeneous SPM distribution
177 along the cross and bottom-up section at moderate flow conditions (Pont et al., 2002). Four
178 250-ml water samples were pumped per day into the same bottle, providing an integrated
179 daily sample. For more details about the design and functioning of the monitoring station, see
180 Pont et al (2002). River samples were collected every month over the course of the three
181 years and covered a broad range of riverine discharge rates (Fig.1) including flood events.
182 Water sub-samples were filtered in the laboratory on Whatman GF/F precombusted quartz
183 filters in an all-glass filter holder and then dried for 24 h at 65°C and weighted to evaluate the
184 total suspended particulate matter before further analysis (organic carbon and $D^{14}C_{POC}$).
185 Further analysis (organic carbon, $\delta^{13}C_{POC}$ and $\Delta^{14}C_{POC}$) were performed on freeze-dried

186 particulate material concentrated after a decantation step (24 h in a 5°C dark room) of the
187 remaining water sample, following by a centrifugation (2000 rpm, 5°C, 5 min).

188 **3.1.2. Sediment and SPM Sampling**

189 Two scientific cruises (Minercot 2 and RiOMar 1) were conducted off the Rhône
190 River mouth in June 2005 and April 2007, respectively. The network of sampling stations
191 (Fig. 1) is described by Lansard et al. (2009) and the locations and water depths are displayed
192 in Tables 1 and 2. The sampling strategy focused on the Rhône River prodelta, with a grid of
193 closely spaced stations (A, B, K). The connection of the Rhône River prodelta with the
194 continental shelf was studied through South-West, South and South-East onshore–offshore
195 transects. The 2 cruises took place during period of average discharge rates of the Rhône
196 River (Cathalot et al., 2010; Lansard et al., 2009).

197 Sediment samples were collected with a multicorer MUC 8/100 (Oktopus GmbH) deployed
198 from the R.V. Téthys II. Eight cores (internal diameter: 9.5 cm) were simultaneously
199 collected and sliced at 1 cm depth intervals. The subsampled sediments were then stored at -
200 20°C until analysis. Sediment samples were freeze-dried and then ground using an agate
201 mortar.

202 In addition, intermediate and bottom waters were collected using Niskin bottles in April 2007
203 (Table 1). Water samples were filtered on Whatman GF/F precombusted quartz filters in an
204 all-glass filter holder. Filters were washed with distilled water to eliminate the remaining salt
205 and immediately frozen on board at -20°C. They were then dried at the laboratory for 24 h at
206 65°C and weighted to evaluate the total suspended particulate matter.

207 **3.2. Organic Carbon Content**

208 Organic Carbon (OC) content was measured in surface sediment (0–1 cm) after inorganic
209 carbon removal by dissolution with a 1% HCl solution. The OC content for the sediments
210 collected in June 2005 were determined at LSCE, using an automatic Fisons Instrument NA
211 1500 Element Analyzer, whereas OC measurements for the sediments sampled in April 2007
212 were performed at CEFREM, by an automatic CHN-analyser LECO[®] 2000. Precisions for OC
213 by both types of analyses were 2% (relative standard deviation).

214 Measurements of POC in bottom and intermediate waters (April 2007) were performed at
215 LSCE using a different decarbonation treatment: filters were acidified with H₃PO₄ (1%)
216 during 24 hours at room temperature (Druffel et al., 1992). The remaining acid was removed
217 by percolating through the filters, which were then dried at 65°C during two days. The
218 precision for OC by this procedure was 3%.

219 **3.3. Stable Isotopic Composition of Organic Carbon**

220 Stable carbon isotope ratios of OC were determined in surface sediment ($\delta^{13}\text{C}_{\text{OC}}$) and SPM
221 ($\delta^{13}\text{C}_{\text{POC}}$) after carbonate removal by acidification. Analysis of the June 2005 samples were
222 performed using a continuous flow ThermoFinnigan Delta Plus XP Isotopic-Ratio Mass
223 Spectrometer (IR-MS). Isotopic signatures of April 2007 sediments were measured at
224 CEFREM on an Isoprime (GVI) IR-MS. An intercomparison between the two IRMSs was
225 performed with 3 decarbonated samples from April 2007. Results showed no significant
226 difference between the $\delta^{13}\text{C}_{\text{OC}}$ values obtained ($p < 0.01$, non parametric Mann-Whitney test).

227 The isotopic compositions were reported using the standard δ -notation (‰) with respect to the
228 Vienna Pee Dee Belemnite (PDB) standard. Isotopic results were obtained with uncertainties
229 of $\pm 0.15\text{‰}$.

230

231 **3.4. Proto-kerogen and Black Carbon fractionation:**

232 Two operationally defined pools of OC were chemically and physically isolated from bulk
233 sediments. The wet procedure described by Song et al. (2002) was used to obtain a proto-
234 kerogen/ black carbon (BC) mixture via acid demineralization, solvent extraction, and base
235 hydrolysis. The procedure described by Gustafsson et al. (2001) was used to obtain pyrogenic
236 BC through thermal oxidation and HCl treatment.

237 Description of the methods used to isolate and quantify the Proto-kerogen/BC mixture, and
238 pyrogenic-graphitic BC are provided as Supplementary material.

240 **3.5. Polycyclic Aromatic Hydrocarbons (PAH) Analysis in the Rhône River Delta** 241 **Sediments**

242 The analysis of the Rhône River delta sediments included different suites of PAHs such as
243 unsubstituted parent compounds, alkyl-substituted homologues (C-PAH) and unsubstituted
244 sulfur heterocycle and their alkyl-substituted compounds (SPA_H and C-SPA_H). The
245 concentrations were determined for more than 40 individual compounds and also group of
246 their alkyl-substituted homologues (Tronczynski et al., 2004). A description of the method is
247 provided as Supplementary material.

248 Quantitative PAH source apportionment was carried on the Rhône River samples together
249 with PAH data determined in surface sediments from the bay of Biscay and the Northwestern
250 Mediterranean Sea (Tronczynski et al., 2004). The source analysis in these sediment samples
251 was constrained to two sources of PAH: i) pyrogenic/combustion, and ii) petroleum /oil
252 residue. Two common mixture analysis approaches were adopted using Alternating Least
253 Squares (ALS) and Multivariate Curve Resolution (MCR) calculation techniques (Larsen and
254 Baker, 2003). Both methods give similar results ($r^2 = 0.98$, $n = 95$) and only ALS results are

255 presented here. Mixture analysis calculation provides PAH source amounts apportionment in
256 each sample as well as PAH source profiles (compositions) estimates (Tauler et al., 1993).

257 **3.6. Lignin-Phenol Analysis**

258 A detail description of the method is provided in the Supplementary Material. Briefly, freeze-
259 dried sediment samples (transect from station A to F) were analyzed for lignin-phenols using
260 the cupric-oxide method (Hedges and Ertel, 1982). Lignin oxidation products were quantified
261 by GC-FID.

262 We quantified eight lignin-derived phenols, unique to vascular plants, and produced during
263 alkaline CuO oxidation. The vanillyl phenol (V) group, consisting of vanillin (Vl), vanillic
264 acid (Vd) and acetovanillone (Vn), is present in all vascular plants. The syringyl group (S),
265 consisting of syringaldehyde (Sl), syringic acid (Sd), and acetosyringone (Sn), are only found
266 in woody and non-woody angiosperms. The cinnamyl phenols, ferulic acid (Fd) and *p*-
267 coumaric acid (*p*-Cd), are only present in non-woody tissues of gymnosperms and
268 angiosperms. In addition, CuO oxidation yields *p*-hydroxybenzenes (P) that are derived from
269 both lignin and non-lignin sources (Goni and Hedges, 1995). Lignin parameters of total
270 syringyl to vanillyl (S/V) and total cinnamyl to vanillyl (C/V) phenols were used to
271 distinguish the relative contributions of plant types (gymnosperm vs. angiosperm) and tissue
272 types (woody vs. non-woody) respectively. Cinnamyl phenols were found to be readily
273 released from herbaceous tissues with a mild-base hydrolysis and exhibit a marked increase in
274 lability relative to the lignin pool, during decomposition (Opsahl and Benner, 1994);
275 therefore, to avoid the large variability in cinnamyl phenol pools and reactivity, the
276 contribution of lignin to the organic matter pool was estimated using the carbon-normalized
277 sum of syringyl and vanillyl phenols, Λ_6 ($\Lambda_6 = S + V$).

278 **3.7. Compound-specific Isotope Analysis of Lignin-Phenols**

279 The compound-specific $\delta^{13}\text{C}$ values of lignin-derived phenols were measured by isotope ratio
280 monitoring-gas chromatography-mass spectrometry (irm-GC-MS). Please see description in
281 Supplementary Material. The $\delta^{13}\text{C}$ value of the lignin pool was estimated by isotopic mass
282 balance of syringyl and vanillyl phenols (equation 1):

$$283 \quad \delta^{13}\text{C}_{\text{S,V}} = \sum f_i \delta_i \quad (1)$$

284 where i represents individual lignin phenols (vanillin, vanillic acid, acetovanillone,
285 syringaldehyde, syringic acid and acetosyringone); f_i represents the fraction of each phenol,
286 and δ_i indicates the $\delta^{13}\text{C}$ value of the corresponding lignin phenol. Errors were calculated
287 following the classical error propagation formula for the linear combination of each phenols
288 contribution (equation 2):

$$289 \quad \text{std}\delta^{13}\text{C}_{\text{S,V}} = (\sum f_i^2 \text{std}\delta_i^2)^{1/2} \quad (2)$$

290 with std designating the error on the $\delta^{13}\text{C}$ value considered.

291

292 **3.8. Radiocarbon Organic Carbon Content**

293 Radiocarbon measurements (^{14}C) were performed either by the Artémis accelerator mass
294 spectrometer (AMS) at the Laboratoire de Mesure du Carbone 14, Gif-sur-Yvette (for
295 sediment samples) or by the NSF - Arizona AMS facility, Tucson (for suspended particles
296 samples). Measurements were performed at two different sediment depths: 0-1 cm and 3-4 cm
297 depth. After the decarbonation, the entire sample was combusted in a sealed quartz tube at
298 850°C with copper oxide and silver wool. The released CO_2 was dried, volumetrically
299 measured, and collected in a glass ampoule. Then, the CO_2 sample was converted to graphite
300 target in an atmosphere of H_2 over an iron powder catalyst at 600°C (Arnold et al., 1989) and

301 the sample $^{14}\text{C}/^{12}\text{C}$ ratio was then measured. The ^{14}C activities are determined with respect to
302 the international standard of oxalic acid and are reported in $\Delta^{14}\text{C}$ (Stuiver and Polach, 1977).
303 The $\Delta^{14}\text{C}$ is defined as the deviation in parts per mil from the modern standard. All $\Delta^{14}\text{C}$
304 values were corrected from 1950, and from the delay between sampling and measurement
305 years (Mook and van der Plicht, 1999). Ages were calculated from the $\Delta^{14}\text{C}$ values using the
306 conventional ^{14}C half-life. The precisions of $\Delta^{14}\text{C}$ measurements were $\pm 3\text{‰}$ for the sediment
307 samples (Artemis AMS) and $\pm 0.2\text{‰}$ for the suspended particles (Arizona AMS facility).
308 Total uncertainties in $\Delta^{14}\text{C}_{\text{OC}}$ are listed in Tables 1 and 2 for each samples.

309 **4. RESULTS:**

310 **4.1. River samples:**

311 The suspended particulate matter (SPM) sampled monthly from 2006 to 2009 in the Rhône
312 River displayed a mean OC content of $1.9 \pm 0.5 \%$, and a $\delta^{13}\text{C}_{\text{POC}}$ mean value of $-27.4\text{‰} \pm$
313 0.7‰ (Table 1). This $\delta^{13}\text{C}_{\text{POC}}$ composition is in agreement with a previous survey on the SPM
314 from the Rhône River, which gave a mean $\delta^{13}\text{C}_{\text{POC}}$ of $-26.8\text{‰} \pm 0.2\text{‰}$ over 2004-2005
315 (Harmelin-Vivien et al., 2010; Harmelin-Vivien et al., 2008) and reflects the dominance of
316 the C_3 photosynthetic pathway within the Rhône River watershed throughout the seasons
317 (Table 1).

318 Over the three years survey, SPM displayed $\Delta^{14}\text{C}_{\text{POC}}$ signatures between 148 and -90‰ ,
319 including period of flood events. Black carbon (BC) contents in the Rhône River SPM were
320 $0.34 \pm 0.12\%$ (d.w.).

321 **4.2. Background Data: Organic Carbon Content**

322 In April 2007, temperatures in bottom and intermediate waters were homogeneous over the
323 entire study area (prodelta and continental shelf), ranging between 14.1 and 15.3°C at depths

324 of 13 to 98 m (Table 1). The SPM contents varied between 0.8 and 5.4 mg L⁻¹, with no
325 significant spatial pattern.

326 The highest POC concentrations were observed near the Rhône River mouth with values
327 ranging between 150 and 266 µgC l⁻¹ (Stations A, K, B, L and N). The POC contents of SPM
328 samples were around 10% at the river mouth and decreased offshore to values around 3%
329 (Table 1). Surface and intermediate waters presented slightly higher POC contents than
330 bottom waters, but given the variability, they were not significantly different (p>0.05).

331 The distribution and values of OC in surface sediment were stable over the two cruises
332 and ranged between 2% at the vicinity of the river mouth and 1% offshore. The OC contents
333 were slightly lower offshore during the June 2005 cruise but the overall prodelta distribution
334 was not significantly different from April 2007 (p>0.05, Table 2, for data in June 2005 see
335 Lansard et al, 2009).

336 **4.3. Stable Carbon Isotopic Composition**

337 The δ¹³C_{OC} values for surface sediments collected in June 2005 are those reported by Lansard
338 et al. (2009). The δ¹³C_{OC} signatures did not show any significant changes between June 2005
339 and April 2007 in surface sediment (p>0.05): values of δ¹³C_{OC} ranged from -27.2‰ at station
340 A (outlet of the river) to -23.9‰ at station J (south-eastward) (Table 2). All δ¹³C_{OC} values
341 increased with distance from the Rhône River mouth (r² = 0.845, n = 27, p<0.01, see Lansard
342 et al., 2009). Stations A, B and K are located within a 2 km radius off the Rhône River mouth
343 and presented strongly depleted δ¹³C_{OC} values around -27 and -26‰, associated with high OC
344 contents (~ 2%). Proceeding offshore, stable carbon isotope ratios rose up to -24‰ at the far
345 most end of the South-West transect and eastern stations, corresponding to the lowest OC
346 contents (~0.8 - 1%).

347 Contrary to surface sediment values, stable carbon isotope ratios of suspended POC ($\delta^{13}\text{C}_{\text{POC}}$)
348 in bottom and intermediate waters were homogeneous in the whole prodelta, with values of -
349 $24.0 \pm 0.3\text{‰}$ in bottom waters and $-23.2 \pm 0.8\text{‰}$ in intermediate waters, respectively (Table
350 1). There was no specific trend in spatial $\delta^{13}\text{C}_{\text{POC}}$ distribution in the prodelta or the
351 continental shelf.

352 **4.4. Distribution of $\Delta^{14}\text{C}_{\text{OC}}$ and $\Delta^{14}\text{C}_{\text{POC}}$**

353 $\Delta^{14}\text{C}_{\text{POC}}$ signatures were measured in SPM from the Rhône River. Samples collected in April
354 2006, March 2007, September and November 2008 and February 2009 displayed $\Delta^{14}\text{C}_{\text{POC}}$
355 values between -90‰ and 148‰ (Table 1).

356 The $\Delta^{14}\text{C}_{\text{OC}}$ signature of surface sediments in the prodelta presented a wide range of values
357 from $+143\text{‰}$ to -400‰ (Table 2). A clear trend was observed with $\Delta^{14}\text{C}_{\text{OC}}$ values decreasing
358 with distance from the Rhône river mouth ($r^2 = 0.942$, $n = 14$, $p < 0.01$, see Fig. 2). Surface
359 sediments in the immediate vicinity of the Rhône River mouth (station A) presented a modern
360 $\Delta^{14}\text{C}_{\text{OC}}$ signature ranging between 59‰ and 143‰ , slightly higher than the current
361 atmospheric $\Delta^{14}\text{C}\text{-CO}_2$ level ($\sim 70\text{‰}$, (Levin and Kromer, 2004)), and around 0‰ at B and K
362 (Fig. 2, Table 2). Moving offshore, the $\Delta^{14}\text{C}_{\text{OC}}$ signatures of sediments decreased rapidly with
363 distance from the Rhône River mouth, down to values around -400‰ in the most distal area,
364 corresponding to an age of about 4000 years BP (Fig. 2; Table 2).

365 Except station A, which was markedly enriched with POC values in SPM of intermediate
366 waters reaching modern carbon values, all stations showed SPM in bottom waters with
367 $\Delta^{14}\text{C}_{\text{POC}}$ lower than -100‰ . Offshore, the $\Delta^{14}\text{C}_{\text{POC}}$ values of SPM decreased very quickly,
368 down to values around -300‰ (Table 1). At the station E, on the continental shelf, the
369 radiocarbon signature of SPM ($\Delta^{14}\text{C}_{\text{POC}}$) was similar to surface sediments $\Delta^{14}\text{C}_{\text{OC}}$ (Table 1).

370 Nevertheless, our results show no correlation between sediment and overlying suspended
371 POC radiocarbon signatures ($p > 0.05$, Table 1 and 2).

372 **4.5. Black Carbon (BC) and Proto-kerogen/BC mixture:**

373 Sediment in the prodelta and the continental shelf display similar Black Carbon (BC)
374 contents, ranging from 0.21 to 0.47% d.w. with a mean $\delta^{13}\text{C}_{\text{OC}}$ value of $-24.6 \pm 0.6\text{‰}$ (Fig. 6).
375 Since OC content in the sediment decrease from the river mouth to the continental shelf (from
376 1.8% to 0.8%), such constant BC values correspond to an increase from 12 to 50% of BC
377 content in OC.

378 On the contrary, the proto-kerogen/BC mixture shows a clear decrease within the transition
379 zone: sediment in the prodelta (stations A, B, K) displayed contents of $0.69 \pm 0.12\%$ d.w.
380 significantly higher than the stations on the continental shelf with values of $0.47 \pm 0.02\%$. In
381 addition, the stable carbon isotopic signature of the proto-kerogen/BC mixture in the prodelta
382 was $-27.5 \pm 0.6\text{‰}$ whereas it was $-25.3 \pm 0.4\text{‰}$ in the continental shelf. The proto-
383 kerogen/BC mixture contribution to OC did not show any clear pattern over the area and was
384 around 40-50% OC.

385 Please note that both fractions were obtained through different technique (chemical or thermal
386 procedure) and the respective contribution of BC and proto-kerogen/BC mixture to OC
387 content should not be compared among one another (Elmquist et al., 2004; Gelinas et al.,
388 2001).

389 **4.6. Lignin-Derived Phenols And Their Stable Carbon Signatures**

390 The average carbon-normalized lignin contents (Λ_6) were similar in the 1-2 cm and the 3-4
391 cm depths and decreased with distance from the river mouth (Table 3). Syringyl and vanillyl
392 phenol contributions were fairly equal (around 50%, Table 3) near the river mouth (station A)
393 but the vanillyl phenol yield increased with offshore transport (Table 3), suggesting a greater

394 contribution of angiosperm tissues in near-shore sediments (Hedges and Mann, 1979b). The
395 relative cinnamyl phenol yields were the lowest, ranging from 4.6% to 11.8% in upper 1-2 cm
396 sediments and 5.6 to 7.2% at 3-4 cm depth. The S/V and C/V ratios at both depths generally
397 decreased with an increased distance from the river mouth (Table 3, Fig. 3). The (Ad/Al)_v
398 ratio of sediments from the Rhône River transect did not significantly vary with offshore
399 distance but nearly a doubling in (P/V+S) was observed (Table 3).

400 $\delta^{13}\text{C}$ values of the syringyl and vanillyl pool ($\delta^{13}\text{C}_{\text{S,V}}$) were consistently lower in sediments at
401 1-2 cm relative to those at 3-4 cm depth. However, there was an increase in the $\delta^{13}\text{C}$ value
402 along the transect at both depths (Table 3). From station A to station E, the $\delta^{13}\text{C}$ value of
403 lignin in surface sediments (1-2 cm) increased by 4.3‰, while those of sediments at 3-4 cm
404 increased by 7.3‰ (Table 3). Despite its rather weak significance level (probably as a result
405 of the low amount of data available), this increase in $\delta^{13}\text{C}_{\text{S,V}}$ along the transect was
406 statistically relevant ($p \leq 0.1$, Kruskal-Wallis).

407 **4.7. PAH in the Rhône Prodelta And Adjacent Continental Shelf.**

408 Summed concentration of total PAHs in the sediment from the Rhône River prodelta and
409 adjacent continental shelf ranged from about 2000 to 2400 $\mu\text{g kg}^{-1}$ (d.w.) and showed no
410 gradient along the dispersal system (Table 4). Results from the Rhosos cruise performed in
411 2008 (Tronczynski, unpublished results) were added as additional PAHs data in surface
412 sediments of the continental shelf. The concentrations of total PAHs normalized to organic
413 carbon ranged from about 110 to 330 mg kg^{-1} OC and were higher at station C (75 m) than at
414 the station A. The levels of summed sedimentary concentrations of six indicators ΣPAH_6
415 ranged from 450 to 600 $\mu\text{g kg}^{-1}$ d.w. (Table 4).

416 The petroleum component is estimated to be 30% (mean ± 1 % $n = 4$) of total PAH in the
417 Rhône delta sediments (Table 4) using mixture analysis calculation by ALS (Grande and

418 Manne, 2000). The remaining 70% originates from fossil fuel and biomass combustion
419 (pyrogenic origin).

420 The total PAH content of the sediment was estimated by using a multiplying factor of 5 on
421 our PAH estimates (Table 4) to account for all sulfur, oxygen and not quantified compounds,
422 as previously used in coastal sediments (Tolosa et al., 1996; Tronczynski et al., 2004). The
423 total PAH concentration in the Rhône River prodelta is thus about 10 mg kg^{-1} dry weight (dw)
424 ($2000 \text{ } \mu\text{g kg}^{-1}$ from Table 4 multiplied by 5).

425 Petroleum PAH fraction represents 30% of the total PAH (Table 4) which leads to a
426 concentration of petroleum residues-PAH of 3 mg kg^{-1} dw. To calculate the petroleum carbon
427 content, we used a conservative value of 20% of PAH in petroleum, since aromatic
428 hydrocarbons significantly vary from one oil (and its refinery products) to another, ranging
429 from 20 to 50% of different oils and refinery products (Lee et al., 1986). The total
430 concentration of oil residue-derived OC in the sediment was therefore estimated to be 15 mg
431 kg^{-1} dw ($3 \text{ mg kg}^{-1}/20\%$).

432 The pyrogenic fraction of PAH is derived from combustion of fossil fuel or biomass and
433 represents 70% of PAH : hence 7 mg kg^{-1} of PAH out of the total of 10 mg kg^{-1} was of
434 pyrogenic origin (i.e. wood chars and soot). The predominance of fossil fuel combustion over
435 residential wood combustion as the major source of pyrogenic BC and associated PAHs was
436 examined by using ratios of 1,7-dimethylphenanthrene to 2,6-dimethylphenanthrene.
437 Expressed as $1,7/(1,7+2,6)$ -DMP, this ratio is known to be less than 0.42 for diesel particles
438 and urban dust, whereas it reaches 0.70-0.90 in emissions from wood combustion (Benner et
439 al., 1995). In sediment from our study area, we found this PAH ratio to be 0.45 implying that
440 about 95% of the pyrolytic PAHs were derived from fossil fuel combustion (Yunker et al.,
441 2012). Neglecting the wood/biomass combustion fraction, we can therefore consider that 7

442 mg kg⁻¹ of PAH out of the total of 10 mg kg⁻¹ originate from fossil fuel combustion (i.e. diesel
443 soot, vehicle emission). In addition, assuming that PAHs represent 5% of the total combustion
444 carbon (White et al., 2005), we can calculate a concentration of pyrogenic BC of 140 mg kg⁻¹.

445

446 **5. DISCUSSION**

447 The radiocarbon signatures, stable carbon isotopic compositions and BC contents presented
448 above indicate that different OC sources contribute to the organic matter in the river and shelf
449 samples (Fig. 5). Additionally, lignin phenols' yields and isotopic signature suggest that a
450 significant fraction of the organic matter exported by the Rhône River is lost during its
451 introduction into the shelf environment. In the following sections, we investigate the sources
452 of the OC pools exported by the Rhône River and the processes affecting their export in the
453 sediments of the Gulf of Lions continental shelf.

454 **5.1. River input of organic matter: variability and signature**

455 The largest source of organic matter to the delta is the Rhône River which is
456 characterized by large variations of discharge (Fig. 1). Flood periods, defined as water
457 discharge rates exceeding 3000 m³ s⁻¹ at Arles gauging station, occur in early spring and late
458 fall and lasts from a few days to a week. These high discharge episodes are known to carry
459 most of the material (about 80%) to the coastal ocean (Antonelli et al., 2004; Roussiez et al.,
460 2005).

461 In this study, six periods characterized by high river discharge (with four floods) were
462 investigated for $\Delta^{14}\text{C}_{\text{POC}}$ whereas $\delta^{13}\text{C}_{\text{POC}}$ was measured every month over the three-year
463 study (January 2006 to February 2009). The time-series shows that the $\delta^{13}\text{C}_{\text{POC}}$ signature of
464 the suspended particles in the Rhône River is relatively stable ($-27.4 \pm 0.7\text{‰}$) during both low

465 discharge and flood events (2006-2008). The Rhône River SPM displayed a variable $\Delta^{14}\text{C}_{\text{POC}}$
466 signature between 147 and -90‰ (average $29 \pm 93\%$, $n=5$, Table 1) which likely reflected the
467 mixing of different terrigenous materials in the River, i.e. fresh plant debris mixed with a low
468 proportion of older soil organic matter. The $\Delta^{14}\text{C}_{\text{POC}}$ signature of the Rhône River could also
469 be influenced by the adjacent nuclear power plants: they can potentially increase the $\Delta^{14}\text{C}_{\text{POC}}$
470 signature in the river (Faurescu et al., 2008). This is contrasting with other RiOMar systems in
471 temperate settings, where ^{14}C signatures of POC are relatively older with $\Delta^{14}\text{C}_{\text{POC}}$ signature
472 ranging from -175‰ down to -550‰ (Raymond and Bauer, 2001a; Wakeham et al., 2009).
473 The $\Delta^{14}\text{C}_{\text{POC}}$ decreased to a low value of -495‰ only one time over the three years of
474 monitoring, in May-June 2008, due to an exceptional flood of the Durance River located in
475 the south-western Alps. This flood was linked to a water release by a dam. Therefore it is
476 likely that during the event the flood wave carried a large amount of fine organic-poor
477 sediments originating from bank erosion. This distinct source of organic matter was also
478 obvious based on the $\delta^{13}\text{C}_{\text{POC}}$ signature (-25.8‰), a value never reached during the 3-year
479 monitoring period. On average, the organic matter supplied to the Rhône River prodelta
480 corresponds to a modern terrestrial material similar to the one observed in the sediment of the
481 shallowest station A located just off the river mouth (24 m water depth).

482

483 **5.2. The River-Shelf transition zone: major changes in particle signature**

484 The input of Rhône River exerts first order control on the composition of sedimentary
485 organic matter located in the prodelta, i.e. near the river mouth. The terrestrial signature of the
486 OM deposited in this zone is progressively altered along the sediment transport pathway
487 along the continental shelf as shown on Fig. 4. We pooled our data with the ones from Tesi et
488 al. (2007) and Tesi et al (2010a; 2010b) who had performed $\delta^{13}\text{C}_{\text{OC}}$, $\Delta^{14}\text{C}_{\text{OC}}$ and lignin

489 measurements in surface sediments further away in the Gulf of Lions continental shelf. The
490 striking feature is the constancy of the particle signature on the entire shelf mud belt (Fig.4).
491 Indeed, the $\Delta^{14}\text{C}_{\text{OC}}$, $\delta^{13}\text{C}_{\text{OC}}$ and OC contents presents less than 6% variation over a western
492 125 km transect across the shelf. Regarding the biogeochemical parameters from this study,
493 70% of the changes occur in the prodelta within a transition zone between the river mouth and
494 the continental shelf. Most transformation, mixing, sorting and degradation processes
495 altering/impacting the material delivered by the Rhône River appeared to occur within this
496 narrow zone of 10 km radius area around the Rhône River mouth. On the contrary, shelf
497 sediments display low organic carbon content, mixed $\delta^{13}\text{C}_{\text{OC}}$ (-24.5‰) and low $\Delta^{14}\text{C}_{\text{OC}}$
498 (around -400‰) with a constant signature over the entire shelf of the Gulf of Lions. These
499 sediments are characteristic of inert particles which are redistributed and mixed on the
500 continental shelf by wind induced currents (Ulses et al., 2008; Estournel et al., 2003; Roussiez
501 et al. 2006).

502 The transition zone displays a continuous gradient of isotopic signature (Fig. 4) with
503 increasing distance from the Rhône River mouth. The shallow Rhône prodelta is a significant
504 zone of retention for riverine particles, e.g. Station A (Table 2) which is located at 2 km from
505 the river mouth at a depth of 24 meters. In addition to high sedimentation rates, it was shown
506 using ^{238}Pu that most particles delivered by the Rhône River were deposited and stored near
507 the Rhône River mouth (Lansard et al., 2007). The isotopic composition of organic carbon in
508 the sediment of station A reflects that of the river with a modern $\Delta^{14}\text{C}_{\text{OC}}$ (+ 60-140‰) and a
509 $\delta^{13}\text{C}_{\text{OC}}$ of -27‰. Furthermore, the large lignin content of the sediment suggests that the
510 organic material is mostly terrestrial. Although this station exhibits the highest mineralization
511 rate of organic matter in the sediment (Cathalot et al., 2010), it is mostly an accumulation
512 centre with a burial efficiency of 80% (Pastor, Cathalot et al., 2011).

513 Stations located further away from the river mouth (B, K, L, N, C) in the transition
514 zone (3-10 km) showed a progressive change of the primary signature of the river particles.
515 $\Delta^{14}\text{C}_{\text{OC}}$ decreases to values as low as -220‰ at station C and $\delta^{13}\text{C}_{\text{OC}}$ increases to -25‰,
516 reflecting the apparent aging of organic carbon and its loss of terrestrial signature,
517 respectively (Fig. 2, Table 2). In this region, several processes may modify the original
518 signature of river particles: (1) selective degradation of relatively young terrestrial organic
519 matter, (2) sorting of particles with different biogeochemical signatures (fossil versus labile
520 carbon with different size/density characteristics (Tesi et al., 2007a), (3) mixing with the pool
521 of old and refractory shelf particles. Mineralization rates are substantial in the sediment of the
522 transition zone (Cathalot et al., 2010) and burial efficiency decreases from 60% (stations B,
523 K, L) to 20% (station E) indicating that a substantial part of organic carbon is processed in
524 these sediments (Pastor et al., 2011a).

525 In the next sections, we discuss the processes and their interplay which may lead to the
526 observed isotopic and biomarkers gradient.

527

528 **5.3. Hydraulic sorting within the prodelta area**

529 Hydraulic transport mechanisms, which preferentially transport the finest material,
530 alter the grain size distribution in surficial sediments (Marion et al., 2010). To assess the
531 impact of grain size distribution on the export of OM in sediment of the Rhône River prodelta
532 and the adjacent continental shelf, we plotted our radiocarbon signatures as a function of the
533 silt/clay fraction content (Pastor et al., 2011b). Figure 7 clearly shows a dual behaviour of
534 $\Delta^{14}\text{C}_{\text{OC}}$ signatures with respect to grain size distribution. In the prodelta, a clear gradient in
535 the $\Delta^{14}\text{C}_{\text{OC}}$ values suggest a loss of a young coarse material in the transition zone (stations A,
536 B, K) as the sediment is being exported towards the continental shelf along the main sediment

537 transport system. This corresponds most likely, to a “fresh” woody material associated with
538 coarse-sized particles preferentially retained close to the river mouth (Tesi et al., 2007a). As a
539 consequence of this initial hydraulic sorting, soil-derived OM bound to the particles and all
540 small size particles are selectively transported further offshore (Tesi et al., 2007a).

541 Soil OM can display a wide range of $\Delta^{14}\text{C}_{\text{OC}}$ signatures ranging from modern to pre-
542 aged values and has been proven to constitute a significant part of the sediment OM in many
543 RiOMar systems (Hedges et al., 1999; Mannino and Harvey, 2000). Nevertheless, the
544 sediment granulometry is homogeneous over the continental shelf (silt and clay < 63 μm
545 fraction: $95.3 \pm 1.0\%$, Fig. 7) and the wide range of $\Delta^{14}\text{C}_{\text{OC}}$ values (-102‰ to -400‰)
546 suggesting a limited grain size sorting after the transition zone. The correlation between
547 $\Delta^{14}\text{C}_{\text{OC}}$ and the particle size fraction < 63 μm ($r^2=0.730$, $n=24$, Fig. 7) disappears when
548 considering only the continental shelf stations ($r^2=0.024$, $n=16$, Fig. 7). Previous studies
549 described the very fine sediment of the continental shelf, demonstrating the presence of an
550 uniform fine-grained mudbank all over the continental shelf (except for littoral
551 sands)(Lansard et al., 2007; Roussiez et al., 2006). As evidenced for other deltaic systems,
552 particle sorting is likely to be responsible for the gradient of radiocarbon values observed in
553 the transition zone by retaining some coarse woody particles in the shallow prodelta
554 (Toussaint et al., accepted). However, over the continental shelf, this process might be of less
555 importance and fails to explain the distribution of $\Delta^{14}\text{C}_{\text{OC}}$ signatures over the continental
556 shelf. Other mechanisms are likely acting along the main sediment transport system.

557 **5.4. Contribution of ancient OC to the continental shelf sediment**

558 The surface sediments of the continental shelf displayed highly depleted $\Delta^{14}\text{C}_{\text{OC}}$ values
559 compared to the prodelta (Fig. 2, Table 2). Radiocarbon values in the continental shelf were
560 about $-310 \pm 66\%$. [The residence time of the OM in the sediment cannot explain this low](#)
561 [\$\Delta^{14}\text{C}_{\text{OC}}\$ values.](#) Indeed, based on the published sedimentation rates (0.1-0.4 cm y^{-1}) and a 10

562 cm mixed layer (Miralles et al., 2005), the average $\Delta^{14}\text{C}_{\text{OC}}$ value of marine phytodetritus in
563 the sediment mixed layer should be around 30‰ : indeed, the $\Delta^{14}\text{C}_{\text{OC}}$ decay of 100 years from
564 an initial fresh marine signature of 50‰ is <15‰ (Hansman et al., 2009; Wang et al., 1998).
565 Even taking into account the potential reservoir age of 400 years for Mediterranean marine
566 waters (Siani et al., 2001), the large difference between the estimated ages and our
567 radiocarbon data (Table 2) showed that most of the carbon in the Rhône River continental
568 shelf is much older than would be expected if it had been derived from contemporarily
569 synthesized sources (e.g., phytoplankton, vascular plants).

570 The heavily depleted values observed on the continental shelf suggested the presence
571 of aged OC, such as kerogens, graphite, petroleum residues or black carbon (Graz et al.,
572 2010). Originating from bedrock-derived kerogen, fossil fuels combustion or oil
573 contamination, fossil OC generally displays a $\Delta^{14}\text{C}_{\text{OC}}$ of around -1000 ‰ (>60 kyr: it
574 contains nearly no ^{14}C (Drenzek et al., 2007; Goni et al., 2005). Indeed, high contributions of
575 ancient carbon sources to river suspended sediments and surface shelf sediments have been
576 observed in other RiOMar systems (Blair et al., 2003; Galy et al., 2008; Galy and Eglinton,
577 2011; Goni et al., 2006; Gordon and Goni, 2004; Masiello and Druffel, 1998; Masiello et al.,
578 1998). Lateral export of this aged fraction can be promoted by both selective transport of aged
579 material sorbed onto fine particles (i.e., winnowing) and selective degradation of fresh OM
580 along the sediment dispersal system (Hedges et al., 1999; Mannino and Harvey, 2000). As a
581 result, the fraction of terrestrially-derived aged OM becomes gradually more important with
582 increasing distance from river mouth.

583 **5.4.1. Oil residue and pyrolytic BC as ancient OC sources**

584 As the Gulf of Lions is an intense transit area for tanker ships, we used the analysis of
585 polycyclic aromatic hydrocarbons (PAHs) to estimate the actual contribution of fossil fuels,
586 biomass/biofuels combustion as well as direct inputs of oil products in our sediment samples

587 (Kumata et al., 2006; Mandalakis et al., 2005; Sheesley et al., 2009; White et al., 2008; White
588 et al., 2005). Levels of ΣPAH_6 in the sediments of the Rhône River delta range from 450 to
589 600 $\mu\text{g kg}^{-1}$ dw (Table 4), yielding a total PAH concentration of 10 mg/kg dw (see result
590 section for calculation). These levels are characteristic of present-day, chronic, intermediary
591 contamination by PAHs of marine sediments located close to the continental loads. Oil
592 residues represent about 30% of total PAHs in the Rhône delta (Table 4) and the remaining
593 70% originates from fossil fuel and biomass combustion (pyrogenic origin).

594 Based on this distribution of PAHs sources, we can provide a rough estimate of ancient OC
595 originating from petroleum and pyrogenic BC. The total oil residue-derived OC in the
596 continental shelf sediment was estimated to be 15 mg kg^{-1} of OC i.e. 0.15% of OC whereas the
597 pyrogenic fraction amounts to 140 mg kg^{-1} , i.e. 1.4% of total OC. A total of 1.5% of OC is
598 found which is consistent with results of Leaute (2008) in the Thau Lagoon, a mediterranean
599 shallow lagoon.

600 Our PAHs measurements provide us with an estimate of the pyrogenic BC and petroleum
601 fraction of ancient OC and indicate a major contribution of oil residues and soots from vehicle
602 combustion. The low proportion of ancient OC originating from petroleum and pyrogenic BC
603 does not support the observed ^{14}C values on the shelf. Indeed, only 2% of ancient OC mixing
604 up with recent organic material would lead to $\Delta^{14}\text{C}_{\text{OC}}$ values of 78‰ in the sediment, when
605 the observed radiocarbon signatures are around -400‰ (Fig 2, Table 2). Another aged source
606 and other processes are needed to explain the old ages of the continental shelf sediments.

607 **5.4.2. Black Carbon and proto-kerogen/BC fossil OC**

608 Since the Rhône river catchment contains a lot of sedimentary rock, the depleted $\Delta^{14}\text{C}_{\text{OC}}$
609 values, the slightly enriched $\delta^{13}\text{C}_{\text{OC}}$ values and the low lignin content observed in the
610 continental shelf sediments could reflect an important contribution of kerogen-BC mixture.
611 Indeed, as stated above, fossil OC is almost completely depleted in ^{14}C and is generally

612 assumed to have a $\Delta^{14}\text{C}_{\text{OC}}$ value of $\sim -1000\text{‰}$ and a $\delta^{13}\text{C}_{\text{OC}}$ signature ranging between -30 and
613 -12‰ (Drenzek et al., 2009; Goni et al., 2005). Such $\Delta^{14}\text{C}_{\text{OC}}$ signature is however a rough
614 estimate since radiocarbon measurements on graphitic BC samples have shown a range of
615 signatures from -800 to -1000‰ (Dickens et al., 2004; Drenzek et al., 2009; Drenzek et al.,
616 2007). Likely, the rather depleted signature ($\Delta^{14}\text{C}_{\text{OC}} \sim -400\text{‰}$) of continental shelf sediments
617 indicate the presence of fossil material, probably inherited from the Rhône River material and
618 preferentially exported along the dispersal transect.

619 As a matter of fact, our data indicate a contribution of BC to OC increasing from 12% at the
620 river mouth to 50% on the continental shelf (Fig. 6). These values, although remarkable, are
621 consistent with measurements carried out by Lim and Cachier (1996) in NW Mediterranean
622 Sea. The authors, based on chemical oxidation and thermal treatments, estimated a BC/TOC
623 ratio of 38%. The large difference between our pyrogenic BC estimates based on PAHs (1.4%
624 of OC) and our BC measurements based on thermal oxidation (12-50% of OC) suggest a high
625 contribution of graphite in BC. Indeed, the Thermal Oxidation method at 375°C applied here
626 can isolate very highly condensed soot-BC and graphite but can also destroy charcoal-BC and
627 kerogen (Elmquist et al., 2004). Therefore, the low PAH/BC ratios indicate that 90-98% of
628 BC would be of graphitic origin. Graphitic C inputs originating from sedimentary rocks
629 erosion occurring in the catchment of the Rhône River would thus deliver high BC fluxes and
630 generate the high contribution of BC observed in the sediment from the prodelta and
631 continental shelf.

632 In parallel, our data show a decrease of the proto-kerogen/BC fraction along the sediment
633 dispersal system indicating a selective degradation of proto-kerogen like-OM as the terrestrial
634 OM delivered by the Rhône River is exported towards the continental shelf. About 20% of
635 proto-kerogen is lost during the export over the prodelta. Adsorption of otherwise labile
636 organic compounds onto minerals can prevent their diagenetic degradation and promoting

637 their subsequent condensation into kerogen (Salmon et al., 2000). During the transport along
638 the transition zone and within the prodelta sediment, selective degradation mechanisms could
639 remove some kerogen-like material, leaving behind mineral matrix protected OM.

640 **5.5. Degradation mechanisms along the sediment dispersal system**

641 A plot of $\Delta^{14}\text{C}_{\text{OC}}$ and $\delta^{13}\text{C}_{\text{OC}}$ values against 1/OC provides us with a mixing model taking into
642 account changes in the bulk concentration of OC (Fig. 8). The $\Delta^{14}\text{C}_{\text{OC}}$ and $\delta^{13}\text{C}_{\text{OC}}$ ordinates at
643 0.5 (max. 2% OC in the shallow prodelta during our study) indicate the loss of a modern-like
644 OC source ($\Delta^{14}\text{C}_{\text{OC}} \sim 59\text{‰}$) with a very light $\delta^{13}\text{C}_{\text{OC}}$ terrestrial signature ($\sim -27\text{‰}$) as OC
645 decreases across the system. This loss certainly reflects the net decomposition of this
646 terrestrial material through degradation processes and the relative accumulation of old BC
647 offshore.

648 In this study, the lignin phenols contents of the sediments were used as another means
649 for investigating the fate and transfer mechanisms of the terrestrial OM delivered by the river
650 to the coastal ocean. First, a plot of S/V vs. C/V ratios (Fig. 3) indicates that angiosperm
651 woody and leaf materials are major sources of lignin in the shallow Rhône River prodelta
652 (station A). However, both S/V and C/V ratios gradually decrease with increasing distance
653 from the prodelta. Variations in these two ratios are likely caused by two processes: (1)
654 differential lignin degradation (Benner et al., 1991; Haddad et al., 1992; Hedges et al., 1988;
655 Opsahl and Benner, 1995); and (2) differential inputs from angiosperm and gymnosperm
656 woody and non-woody tissue (Hedges and Mann, 1979a).

657 We used lignin stable carbon isotopes to discriminate terrestrial OM between C3 and
658 C4 plant sources. Indeed, C3 plants yield lignin phenols with $\delta^{13}\text{C}$ values $\leq -27\text{‰}$ while C4
659 plants yield lignin phenols with $\delta^{13}\text{C}$ values ranging from -13 to -19 ‰ (Goni et al., 1997). In
660 the shallow prodelta sediments (station A), integrated lignin isotopic compositions ($\delta^{13}\text{C}_{\text{S,V}}$)

661 are below -30‰ (Table 3), clearly indicating a C3-plant origin. However, the $\delta^{13}\text{C}_{\text{S,V}}$ values
662 of the syringyl and vanillyl lignins increase by $\sim 5\%$ from station A to station E (Table 3).
663 The alteration of lignin ^{13}C with increasing distance from the river mouth can be caused by an
664 increase in contribution from C4-derived OM or lignin degradation. The S/V and C/V ratios
665 indicate that gymnosperm-derived lignin accounts for a dominating fraction in off-shore
666 sediments (Fig. 3; see above). Since no gymnosperm plants utilize the C4 photosynthetic
667 pathway (Ehleringer et al., 1997), an increase in contribution from C4-derived OM is unlikely
668 important for the isotopic alteration of lignins in off-shore sediments. Therefore, both lignin
669 phenols and lignin stable carbon isotopes indicate significant lignin degradation over the
670 transition zone.

671 Lignin is generally degraded via propyl side chain oxidation, demethylation of the
672 methoxyl groups, and aromatic ring cleavage (Benner et al., 1991; Ertel and Hedges, 1984).
673 Lignin-derived acid to aldehyde ratio (Ad/Al)_v or (Ad/Al)_s has been used as an indicator of
674 propyl side chain oxidation (Hedges et al., 1988; Opsahl and Benner, 1995). Demethylation
675 results in selective loss of methoxyl groups (vanillyl and syringyl phenols) but does not affect
676 non-methoxylated phenols (p-hydroxyl phenols). Thus, the methoxylated- to non-
677 methoxylated phenol [P/(V+S)] ratio can also be used as a diagenetic indicator of lignin
678 (Dittmar and Lara, 2001; Dittmar et al., 2001). However, p-hydroxyl phenols are derived from
679 a variety of lignin and non-lignin materials, limiting the applications of the [P/(V+S)] ratio.
680 The ratio of p-hydroxyacetophenone (PON) to total p-hydroxyl phenols (PON/P) can be used
681 as an indicator to determine the source of this phenol group (Benner et al., 1990). When
682 aromatic ring cleavage is a dominating pathway for lignin degradation, neither (Ad/Al) nor
683 P/(V+S) ratio can be elevated (Dittmar and Lara, 2001). Our lignin data (Table 3) show that
684 the (PON)/P ratios remain almost constant despite a remarkable decrease of total p-hydroxyl
685 phenols from the prodelta to the shelf, indicating that the sources of this phenol group at

686 different sampling sites are the same and the PON has a reactivity similar to total p-hydroxyl
687 phenols decomposition. Based on this, P/(V+S) ratios can be reliably used as an indicator for
688 lignin degradation. In fact, we observed a doubling in P/(V+S) in offshore versus river mouth
689 sediments while little changes are observed in (Ad/Al)_v, suggesting that lignin becomes
690 increasingly degraded with off-shore transport, mainly via a demethylation pathway. In
691 addition, there is evidence that isotopic compositions of lignin compounds can be altered
692 during degradation processes (Bahri et al., 2008). So, the degradation of lignin along the
693 dispersal sediment system is likely responsible for the alteration in isotopic signature of lignin
694 that we see in the transition zone.

695 Degradation of OM in sediments from the Rhône River estuary to continental shelf
696 has been demonstrated using different proxies. For example, two independent indexes based
697 on amino acid (Dauwe's Index Dauwe et al., 1999) and pigments (ratio of intact chlorophyll-a
698 to the sum of chlorophyll-a + phaeopigments) consistently indicate an increase in degradation
699 state of OM along the transect (Pastor et al., 2011a; Bourgeois et al., 2011). The terrestrial
700 material in Rhône River is largely composed of fresh and labile material (Cathalot et al.,
701 2010; Pastor et al., 2011a), as indicated by the modern $\Delta^{14}\text{C}_{\text{OC}}$ signatures observed at the river
702 mouth, and its lability appears to drive degradation processes in the Rhône River prodelta.
703 Indeed, the increase in degradation state of OM in the prodelta and the adjacent shelf is
704 correlated with the decrease of both terrestrial biomarkers (fatty acids and chlorophyll-b) and
705 benthic mineralization rates (Cathalot et al., 2010). Our radiocarbon data are significantly
706 correlated with the Dauwe Index from Bourgeois et al (2011) ($r^2=0.89$, $p<0.005$), suggesting
707 that the distribution of $\Delta^{14}\text{C}_{\text{OC}}$ signatures is directly related to the degradation processes.

708 Changes in OM composition during the offshore transport due to selective
709 stabilization and degradation of organic compounds can be a predominant feature in the OM
710 cycling of RiOMar systems (Goni et al., 2005; Zonneveld et al., 2010). Our data suggest that,

711 along its dispersion offshore, the OM is selectively degraded with fresh material and proto-
712 kerogen OM being removed through degradation processes, as evidenced by biomarkers and
713 oxygen demand of the sediment (Bourgeois et al., 2011; Cathalot et al., 2010). The OM on the
714 shelf corresponds to a degraded “aged” OM, which will then remain on the continental shelf
715 and be further exported or reworked. If the input of terrestrial organic matter in this system is
716 obvious, the proportion of marine OM is an open question.

717 **5.6. Inputs of fresh marine Organic Matter**

718 In addition to the selective degradation processes occurring along the main dispersal
719 system, many studies in deltaic environments have shown that isotopic and biogeochemical
720 characteristics of POM result from the dilution of the terrestrial material with freshly
721 produced marine phytoplankton (Fry and Sherr, 1984; Hedges et al., 1997; Tesi et al., 2007b).
722 To assess if such dilution processes could explain the radiocarbon signatures observed in the
723 sediments of the Gulf of Lions continental shelf, we applied a three end-members mixing
724 model to our Gulf of Lions sites based on isotopic composition ($\Delta^{14}\text{C}_{\text{OC}}$, $\delta^{13}\text{C}_{\text{OC}}$), and lignin
725 contents (Λ_6). This model has two contemporary terrestrial and marine sources, and a
726 kerogen-BC source (Fig. 5 and 9). Marine phytoplankton, exempt of lignin, was assumed to
727 display a $\Delta^{14}\text{C}_{\text{OC}}$ signature following the $\Delta^{14}\text{C}_{\text{DIC}}$ values ($\sim 100 - 120\%$) of the Mediterranean
728 Sea surface waters (Yechieli et al., 2001) and $\delta^{13}\text{C}_{\text{OC}}$ signatures were taken from Harmelin-
729 Vivien et al. (2008). The parameters for the two contemporary and kerogen-BC terrestrial
730 end-members were taken from both our isotopic measurements and values from the literature.
731 Based on these end-members, we show that sediment of the continental shelf would need a
732 contribution of 30%, 40% and 30% of fresh terrestrial material from the Rhône River,
733 kerogen-BC and fresh marine OM respectively (Fig. 9).

734 The mixing model clearly indicates a gradient of increasing contributions of marine
735 OM and kerogen-BC mixture along the dispersal axis. Immediately after the transition zone,

736 the model-based contribution of kerogen-BC to OC increases from 10% in the prodelta to
737 ~40% all over the continental shelf (station C and E): this is in good agreement with our BC
738 data (Fig. 6) confirming that the material delivered by the Rhône River consists of fossil OC
739 (kerogen-BC mixture) mixed with a fresh terrestrial material quickly deposited within the
740 prodelta. The fossil OC is exported to the continental shelf, reaching 50% of OC in the Gulf
741 of Lions.

742 Similarly, the model-based marine fraction increases along the dispersal gradient from
743 ~10% in the prodelta up to 30% over the continental shelf. This aspect is rather surprising
744 since many proxies in the literature show no increase in labile marine OM over the
745 continental shelf (Bourgeois et al., 2011; Pastor et al., 2011b). In addition, primary
746 productivity within the Rhône River plume and over the continental shelf is rather low (Conan
747 et al., 1998; Lefevre et al., 1997), in agreement with the gradient of mineralization activity
748 along the dispersal transect which is governed by the fresh terrestrial inputs of the Rhône
749 River in the prodelta (Cathalot et al., 2010) rather than inputs of fresh marine OM on the
750 continental shelf. There is a clear discrepancy between our mixing model results and the
751 biomarkers/mineralization features evidenced in previous studies. Likely, the presence of 30%
752 of fresh marine OM in the continental shelf sediment as predicted by the mixing model is an
753 overestimation. Reconciling these two approaches will require a better definition of the end-
754 members of the model (i.e. OC sources) and the processes involved along the main dispersal
755 transect.

756

757 **5.7. Resuspension on the continental shelf**

758 Although the accumulation of old BC-like carbon, dilution with fresh marine OM, and the
759 mechanism of selective degradation of fresh terrestrial OM can explain the biomarker,
760 isotopic and the age signature of OC in the continental shelf, some puzzling factors remain in

761 the understanding of the system. The decrease of OM quality/freshness is not obvious on all
762 biochemical markers: the Enzymatically Hydrolysable / Total Hydrolysable Amino Acids
763 ratios (EHAA/THAA), a proxy for degradation processes in the sediment, shows little
764 decrease along the offshore transect (Pastor et al., 2011b). Other striking features are the
765 homogeneity of the $\delta^{13}\text{C}_{\text{POC}}$ composition of the SPM over the entire prodelta ($-23.7 \pm 0.6\text{‰}$),
766 their depleted $\Delta^{14}\text{C}_{\text{POC}}$ signature (apart of station A), and their similarity with continental
767 shelf sediments (see Tables 1 and 2, and Tesi et al., 2010).

768 These observations suggest that besides selective transport and accumulation of refractory
769 BC-type OM, other mechanisms may be active in the transition zone. Resuspension, transport
770 and redeposition of shelf sediments, consisting in a mixture of old marine OM and BC-
771 kerogen material originating from the Rhône River, is one possible explanation which could
772 contribute to the rapid apparent aging of river particles observed in the River prodelta by
773 differential mixing with deposited shelf sediment. Intense resuspension events, associated
774 with southeasterly storms, are frequent and repeated phenomena affect the inner-shelf
775 sediment of the Gulf of Lions (Estournel et al., 2003; Ulses et al., 2008). Recent work
776 performed on density-fractionated sediments (Toussaint et al., accepted) show that all density
777 fractions from sediments located on the offshore gradient evolve in a similar way. This may
778 be an indication of homogeneous mixing between shelf particles and sediments in the
779 transition zone.

780 **6. CONCLUSION**

781 This study, based on radiocarbon, stable carbon isotopes, lignin phenols, Black Carbon
782 and PAHs analyses, brings new insights on the origin of the organic particulate material on
783 the Mediterranean continental shelf influenced by the Rhône River. In particular, $\Delta^{14}\text{C}_{\text{OC}}$
784 signatures indicate an important pool of aged OC in the continental shelf. Our data indicate an

785 important contribution of BC over the continental shelf. Selective degradation mechanisms
786 along with coarse sediment trapping in the nearshore area promote the removal of fresh
787 terrestrial organic matter but also kerogen-like OM delivered by the Rhône River, as it is
788 exported off the prodelta. Clearly, degradation processes of OM plays a critical role in the
789 aging of OM on the continental shelf off the Rhône River: entangled with OM deposition
790 patterns, oxygen exposure time and benthic mineralization efficiencies, they are the results of
791 an intricate interplay between the OM stock and fluxes in the system. Recent marine organic
792 matter is hardly visible in biomarkers but a mixing model based on C isotopes and lignin
793 indicate that it may constitute a significant proportion of OM in the sediment. An alternative
794 model would be a resuspension/deposition/degradation loop for terrestrial and marine organic
795 matter on the continental shelf which would mix with the sediment of the transition zone
796 contributing to the large $\Delta^{14}\text{C}$ gradient over the area.

797

798

799

800

801 ACKNOWLEDGMENTS:

802 We thank the captains and crews of the R. V. Tethys II for their help during the two scientific
803 cruises of this project. We would like to thank B. Bombled, E. Kaltnecker, C. Hatte, G.
804 Gontier for their work and technical support during the cruises and laboratory analyses. We
805 thank F. Eyrolle for providing us SPM samples collected in the Rhône River during the flood
806 of June 2008.

807 We thank Robert C. Aller and Miguel Goñi for proofreading our article and improving the
808 quality of this manuscript from its early stage to its more final version. This work was
809 supported by the French National Research Agency, programme “Vulnérabilités: Milieux et
810 Climat”, under the grant no. ANR-06-VULN-001 to the CHACCRA project, the French
811 INSU-EC2CO program RiOMar.fr, the MISTRALS/Mermex programme and the CEA. This
812 is a contribution ISMAR XXX. This is LSCE contribution XXX.

813

814 References:

815 Arnold, M., Bard, E., Maurice, P., Valladas, H., Duplessy, J.C., 1989. ^{14}C dating with the Gif-
816 sur-Yvette Tandem Accelerator - Status report and study of isotopic fractionation in the
817 sputter ion-source. *Radiocarbon* 31, 284-291.

818 Bahri, H., Rasse, D.P., Rumpel, C., Dignac, M.F., Bardoux, G., Mariotti, A., 2008. Lignin
819 degradation during a laboratory incubation followed by C-13 isotope analysis. *Soil Biology &*
820 *Biochemistry* 40, 1916-1922.

821 Benner, R., Fogel, M.L., Sprague, E.K., 1991. Diagenesis of belowground biomass of
822 *Spartina-Alterniflora* in salt-marsh sediments. *Limnol. Oceanogr.* 36, 1358-1374.

823 Benner, R., Weliky, K., Hedges, J.I., 1990. Early diagenesis of mangrove leaves in a tropical
824 estuary - molecular-level analyses of neutral sugars and lignin-derived phenols. *Geochim.*
825 *Cosmochim. Acta* 54, 1991-2001.

826 Berner, R.A., 1990. Atmospheric carbon dioxide levels over phanerozoic time. *Science* 249,
827 1382-1386.

828 Bianchi, T.S., Allison, M.A., 2009. Large-river delta-front estuaries as natural "recorders" of
829 global environmental change. *Proceedings of the National Academy of Sciences of the United*
830 *States of America* 106, 8085-8092.

831 Blair, N.E., Leithold, E.L., Ford, S.T., Peeler, K.A., Holmes, J.C., Perkey, D.W., 2003. The
832 persistence of memory: The fate of ancient sedimentary organic carbon in a modern
833 sedimentary system. *Geochim. Cosmochim. Acta* 67, 63-73.

834 Borges, A.V., 2005. Do we have enough pieces of the jigsaw to integrate CO₂ fluxes in the
835 coastal ocean? *Estuaries* 28, 3-27.

836 Bourgeois, S., Pruski, A.M., Sun, M.-Y., Buscail, R., Lantoiné, F., Vétion, G., Rivière, B.,
837 Charles, F., 2011. Distribution and lability of land-derived organic matter in the surface

838 sediments of the Rhône prodelta and the adjacent shelf (Mediterranean sea, France): a multi
839 proxy study. *Biogeosciences Discuss.* 8, 3353-3402.

840 Cathalot, C., Rabouille, C., Pastor, L., Deflandre, B., Viollier, E., Buscail, R., Gremare, A.,
841 Treignier, C., Pruski, A., 2010. Temporal variability of carbon recycling in coastal sediments
842 influenced by rivers: assessing the impact of flood inputs in the Rhone River prodelta.
843 *Biogeosciences* 7, 1187-1205.

844 Charmasson, S., Bouisset, P., Radakovitch, O., Pruchon, A.S., Arnaud, M., 1998. Long-core
845 profiles of Cs-137, Cs-134, Co-60 and Pb-210 in sediment near the Rhone River
846 (Northwestern Mediterranean Sea). *Estuaries* 21, 367-378.

847 Conan, P., Pujon-Pay, M., Raimbault, P., Leveau, M., 1998. Hydrological and biological
848 variability in the Gulf of Lions. II. Productivity on the inner edge of the North Mediterranean
849 Current. *Oceanol. Acta* 21, 767-782.

850 Dagg, M., Benner, R., Lohrenz, S., Lawrence, D., 2004. Transformation of dissolved and
851 particulate materials on continental shelves influenced by large rivers: plume processes. *Cont.*
852 *Shelf Res.* 24, 833-858.

853 Dauwe, B., Middelburg, J.J., Van Rijswijk, P., Sinke, J., Herman, P.M.J., Heip, C.H.R., 1999.
854 Enzymatically hydrolyzable amino acids in North Sea sediments and their possible
855 implication for sediment nutritional values. *Journal of Marine Research* 57, 109-134.

856 De Madron, X.D., Abassi, A., Heussner, S., Monaco, A., Aloisi, J.C., Radakovitch, O.,
857 Giresse, P., Buscail, R., Kerherve, P., 2000. Particulate matter and organic carbon budgets for
858 the Gulf of Lions (NW Mediterranean). *Oceanol. Acta* 23, 717-730.

859 de Madron, X.D., Denis, L., Diaz, F., Garcia, N., Guieu, C., Grenz, C., Loye-Pilot, M.D.,
860 Ludwig, W., Moutin, T., Raimbault, P., Ridame, C., 2003. Nutrients and carbon budgets for
861 the Gulf of Lion during the Moogli cruises. *Oceanol. Acta* 26, 421-433.

862 Dickens, A.F., Gelinas, Y., Masiello, C.A., Wakeham, S., Hedges, J.I., 2004. Reburial of
863 fossil organic carbon in marine sediments. *Nature* 427, 336-339.

864 Dittmar, T., Lara, R.J., 2001. Molecular evidence for lignin degradation in sulfate-reducing
865 mangrove sediments (Amazonia, Brazil). *Geochim. Cosmochim. Acta* 65, 1417-1428.

866 Dittmar, T., Lara, R.J., Kattner, G., 2001. River or mangrove? Tracing major organic matter
867 sources in tropical Brazilian coastal waters. *Mar. Chem.* 73, 253-271.

868 Drenzek, N.J., Huguen, K.A., Montlucon, D.B., Southon, J.R., dos Santos, G.M., Druffel,
869 E.R.M., Giosan, L., Eglinton, T.I., 2009. A new look at old carbon in active margin
870 sediments. *Geology* 37, 239-242.

871 Drenzek, N.J., Montlucon, D.B., Yunker, M.B., Macdonald, R.W., Eglinton, T.I., 2007.
872 Constraints on the origin of sedimentary organic carbon in the Beaufort Sea from coupled
873 molecular C-13 and C-14 measurements. *Mar. Chem.* 103, 146-162.

874 Druffel, E.R.M., Bauer, J.E., Griffin, S., 2005. Input of particulate organic and dissolved
875 inorganic carbon from the Amazon to the Atlantic Ocean. *Geochem. Geophys. Geosyst.* 6.

876 Druffel, E.R.M., Williams, P.M., 1991. Radiocarbon in seawater and organisms from the
877 Pacific coast of Baja-California. *Radiocarbon* 33, 291-296.

878 Druffel, E.R.M., Williams, P.M., Bauer, J.E., Ertel, J.R., 1992. Cycling of dissolved and
879 particulate organic matter in the open ocean. *Journal of Geophysical Research-Oceans* 97,
880 15639-15659.

881 Ehleringer, J.R., Cerling, T.E., Helliker, B.R., 1997. C-4 photosynthesis, atmospheric CO₂
882 and climate. *Oecologia* 112, 285-299.

883 Elmquist, M., Gustafsson, O., Andersson, P., 2004. Quantification of sedimentary black
884 carbon using the chemothermal oxidation method: an evaluation of ex situ pretreatments and
885 standard additions approaches. *Limnol. Oceanogr. Meth.* 2, 417-427.

886 Ertel, J.R., Hedges, J.I., 1984. The lignin component of humic substances - distribution
887 among soil and sedimentary humic, fulvic and base-insoluble fractions. *Geochim.*
888 *Cosmochim. Acta* 48, 2065-2074.

889 Estournel, C., Broche, P., Marsaleix, P., Devenon, J.L., Auclair, F., Vehil, R., 2001. The
890 Rhone river plume in unsteady conditions: Numerical and experimental results. *Estuar. Coast.*
891 *Shelf Sci.* 53, 25-38.

892 Estournel, C., de Madron, X.D., Marsaleix, P., Auclair, F., Julliand, C., Vehil, R., 2003.
893 Observation and modeling of the winter coastal oceanic circulation in the Gulf of Lion under
894 wind conditions influenced by the continental orography (FETCH experiment). *Journal of*
895 *Geophysical Research-Oceans* 108.

896 Faurescu, I., Varlam, C., Stefanescu, C., Vagner, I., Faurescu, D., 2008. Radiocarbon
897 measurements in romanian Danube River water, in: Eikenberg, J., Jäggi, M., Beer, H.,
898 Baehrle, H. (Eds.), *LSC 2008, Advances in Liquid Scintillation Spectrometry*, 1st edition
899 (September 18, 2009) ed. *Radiocarbon*, Davos, Switzerland, pp. 339–344.

900 Fry, B., Sherr, E.B., 1984. $\delta^{13}\text{C}$ measurements as indicators of carbon flow in marine and
901 fresh-water ecosystems. *Contributions in Marine Science* 27, 13-47.

902 Galy, V., Beyssac, O., France-Lanord, C., Eglinton, T., 2008. Recycling of Graphite During
903 Himalayan Erosion: A Geological Stabilization of Carbon in the Crust. *Science* 322, 943-945.

904 Galy, V., Eglinton, T., 2011. Protracted storage of biospheric carbon in the Ganges-
905 Brahmaputra basin. *Nature Geoscience* 4, 843-847.

906 Galy, V., France-Lanord, C., Beyssac, O., Faure, P., Kudrass, H., Palhol, F., 2007. Efficient
907 organic carbon burial in the Bengal fan sustained by the Himalayan erosional system. *Nature*
908 450, 407-410.

909 Gelinas, Y., Prentice, K.M., Baldock, J.A., Hedges, J.I., 2001. An improved thermal oxidation
910 method for the quantification of soot/graphitic black carbon in sediments and soils.
911 *Environmental Science & Technology* 35, 3519-3525.

912 Goni, M.A., Hedges, J.I., 1995. Sources and reactivities of marine-derived organic matter in
913 coastal sediments as determined by alkaline CuO oxidation. *Geochim. Cosmochim. Acta* 59,
914 2965-2981.

915 Goni, M.A., Monacci, N., Gisewhite, R., Ogston, A., Crockett, J., Nittrouer, C., 2006.
916 Distribution and sources of particulate organic matter in the water column and sediments of
917 the Fly River Delta, Gulf of Papua (Papua New Guinea). *Estuar. Coast. Shelf Sci.* 69, 225-
918 245.

919 Goni, M.A., Ruttenger, K.C., Eglinton, T.I., 1997. Source and contribution of terrigenous
920 organic carbon to surface sediments in the Gulf of Mexico. *Nature* 389, 275-278.

921 Goni, M.A., Yunker, M.B., Macdonald, R.W., Eglinton, T.I., 2005. The supply and
922 preservation of ancient and modern components of organic carbon in the Canadian Beaufort
923 Shelf of the Arctic Ocean. *Mar. Chem.* 93, 53-73.

924 Gordon, E.S., Goni, M.A., 2004. Controls on the distribution and accumulation of terrigenous
925 organic matter in sediments from the Mississippi and Atchafalaya river margin. *Mar. Chem.*
926 92, 331-352.

927 Grande, B.V., Manne, R., 2000. Use of convexity for finding pure variables in two-way data
928 from mixtures. *Chemometrics and Intelligent Laboratory Systems* 50, 19-33.

929 Graz, Y., Di-Giovanni, C., Copard, Y., Laggoun-Defarge, F., Boussafir, M., Lallier-Verges,
930 E., Baillif, P., Perdereau, L., Simonneau, A., 2010. Quantitative palynofacies analysis as a
931 new tool to study transfers of fossil organic matter in recent terrestrial environments. *Int. J.*
932 *Coal Geol.* 84, 49-62.

933 Haddad, R.I., Newell, S.Y., Martens, C.S., Fallon, R.D., 1992. Early diagenesis of lignin-
934 associated phenolics in the salt-marsh grass *Spartina-Alterniflora*. *Geochim. Cosmochim.*
935 *Acta* 56, 3751-3764.

936 Hansman, R.L., Griffin, S., Watson, J.T., Druffel, E.R.M., Ingalls, A.E., Pearson, A.,
937 Aluwihare, L.I., 2009. The radiocarbon signature of microorganisms in the mesopelagic
938 ocean. *Proceedings of the National Academy of Sciences of the United States of America*
939 106, 6513-6518.

940 Harmelin-Vivien, M., Dierking, J., Bănar, D., Fontaine, M., Arlhac, D., 2010. Seasonal
941 variation in stable C and N isotope ratios of the Rhone River inputs to the Mediterranean Sea
942 (2004–2005). *Biogeochemistry*.

943 Harmelin-Vivien, M., Loizeau, V., Mellon, C., Beker, B., Arlhac, D., Bodiguel, X., Ferraton,
944 F., Hermand, R., Philippon, X., Salen-Picard, C., 2008. Comparison of C and N stable isotope
945 ratios between surface particulate organic matter and microphytoplankton in the Gulf of Lions
946 (NW Mediterranean). *Cont. Shelf Res.* 28, 1911-1919.

947 Hartnett, H.E., Keil, R.G., Hedges, J.I., Devol, A.H., 1998. Influence of oxygen exposure time
948 on organic carbon preservation in continental margin sediments. *Nature* 391, 572-574.

949 Hedges, J.I., 1992. Global biogeochemical cycles: progress and problems. *Mar. Chem.* 39, 67-
950 93.

951 Hedges, J.I., Blanchette, R.A., Weliky, K., Devol, A.H., 1988. Effects of fungal degradation
952 on the CuO oxidation-products of lignin - A controlled laboratory study. *Geochim.*
953 *Cosmochim. Acta* 52, 2717-2726.

954 Hedges, J.I., Clark, W.A., Quay, P.D., Richey, J.E., Devol, A.H., Santos, U.D., 1986a.
955 Compositions and fluxes of particulate organic material in the Amazon River. *Limnol.*
956 *Oceanogr.* 31, 717-738.

957 Hedges, J.I., Ertel, J.R., 1982. Characterization of lignin by gas capillarity chromatography of
958 cupric oxide oxidation-products. *Analytical Chemistry* 54, 174-178.

959 Hedges, J.I., Ertel, J.R., Quay, P.D., Grootes, P.M., Richey, J.E., Devol, A.H., Farwell, G.W.,
960 Schmidt, F.W., Salati, E., 1986b. Organic ¹⁴C in the Amazon River system. *Science* 231,
961 1129-1131.

962 Hedges, J.I., Hu, F.S., Devol, A.H., Hartnett, H.E., Tsamakis, E., Keil, R.G., 1999.
963 Sedimentary organic matter preservation: A test for selective degradation under oxic
964 conditions. *Am. J. Sci.* 299, 529-555.

965 Hedges, J.I., Keil, R.G., 1995. Sedimentary Organic-Matter Preservation - An Assessment
966 And Speculative Synthesis. *Mar. Chem.* 49, 81-115.

967 Hedges, J.I., Keil, R.G., Benner, R., 1997. What happens to terrestrial organic matter in the
968 ocean? *Organic Geochemistry* 27, 195-212.

969 Hedges, J.I., Mann, D.C., 1979a. Characterization of plant tissues by their lignin oxydation
970 products. *Geochim. Cosmochim. Acta* 43, 1803-1807.

971 Hedges, J.I., Mann, D.C., 1979b. Lignin geochemistry of marine sediments from the Southern
972 Washington Coast. *Geochim. Cosmochim. Acta* 43, 1809-1818.

973 Kumata, H., Uchida, M., Sakuma, E., Uchida, T., Fujiwara, K., Tsuzuki, M., Yoneda, M.,
974 Shibata, Y., 2006. Compound class specific C-14 analysis of polycyclic aromatic
975 hydrocarbons associated with PM10 and PM1.1 aerosols from residential areas of suburban
976 Tokyo. *Environmental Science & Technology* 40, 3474-3480.

977 Lansard, B., Charmasson, S., Gasco, C., Anton, M.P., Grenz, C., Arnaud, M., 2007. Spatial
978 and temporal variations of plutonium isotopes (Pu-238 and Pu-239,Pu-240) in sediments off
979 the Rhone River mouth (NW Mediterranean). *Sci. Total Environ.* 376, 215-227.

980 Lansard, B., Rabouille, C., Denis, L., Grenz, C., 2009. Benthic remineralization at the land-
981 ocean interface: A case study of the Rhone River (NW Mediterranean Sea). *Estuar. Coast.*
982 *Shelf Sci.* 81, 544-554.

983 Larsen, R.K., Baker, J.E., 2003. Source apportionment of polycyclic aromatic hydrocarbons
984 in the urban atmosphere: A comparison of three methods. *Environmental Science &*
985 *Technology* 37, 1873-1881.

986 Leaute, F., 2008. Biogéochimie des contaminants organiques HAP, PCB et pesticides
987 organochlorés dans les sédiments de l'étang de Thau, Sciences de l'environnement d'Ile de
988 France - Marine Biogeochemistry. Université Pierre et Marie Curie, Paris, p. 255.

989 Lee, S.W., Preto, F., Hayden, A.C.S., 1986. Determination of fuel aromatic content and its
990 effect on residential oil combustion. *Abstr. Pap. Am. Chem. Soc.* 192, 42-PETR.

991 Lefevre, D., Minas, H.J., Minas, M., Robinson, C., Williams, P.J.L., Woodward, E.M.S.,
992 1997. Review of gross community production, primary production, net community production
993 and dark community respiration in the Gulf of Lions. *Deep-Sea Research Part II-Topical*
994 *Studies In Oceanography* 44, 801-&.

995 Levin, I., Kromer, B., 2004. The tropospheric (CO₂)-C-14 level in mid-latitudes of the
996 Northern Hemisphere (1959-2003). *Radiocarbon* 46, 1261-1272.

997 Ludwig, W., Meybeck, M., Abousamra, F., 2003. Riverine transport of water, sediments, and
998 pollutants to the Mediterranean Sea, UNEP MAP Technical Report Series. UNEP/MAP,
999 Athens, p. 111.

1000 Maillet, G.M., Vella, C., Berne, S., Friend, P.L., Amos, C.L., Fleury, T.J., Normand, A.,
1001 2006. Morphological changes and sedimentary processes induced by the December 2003
1002 flood event at the present mouth of the Grand Rhone River (southern France). *Mar. Geol.* 234,
1003 159-177.

1004 Mandalakis, M., Gustafsson, O., Alsberg, T., Egeback, A.L., Reddy, C.M., Xu, L., Klanova,
1005 J., Holoubek, I., Stephanou, E.G., 2005. Contribution of biomass burning to atmospheric
1006 polycyclic aromatic hydrocarbons at three European background sites. *Environmental Science*
1007 *& Technology* 39, 2976-2982.

1008 Mannino, A., Harvey, H.R., 2000. Terrigenous dissolved organic matter along an estuarine
1009 gradient and its flux to the coastal ocean. *Organic Geochemistry* 31, 1611-1625.

1010 Marion, C., Dufois, F., Arnaud, M., Vella, C., 2010. In situ record of sedimentary processes
1011 near the Rhone River mouth during winter events (Gulf of Lions, Mediterranean Sea). *Cont.*
1012 *Shelf Res.* 30, 1095-1107.

1013 Masiello, C.A., Druffel, E.R.M., 1998. Black carbon in deep-sea sediments. *Science* 280,
1014 1911-1913.

1015 Masiello, C.A., Druffel, E.R.M., Bauer, J.E., 1998. Physical controls on dissolved inorganic
1016 radiocarbon variability in the California Current. *Deep-Sea Research Part II-Topical Studies*
1017 *in Oceanography* 45, 617-642.

1018 McKee, B.A., Aller, R.C., Allison, M.A., Bianchi, T.S., Kineke, G.C., 2004. Transport and
1019 transformation of dissolved and particulate materials on continental margins influenced by
1020 major rivers: benthic boundary layer and seabed processes. *Cont. Shelf Res.* 24, 899-926.

1021 Megens, L., van der Plicht, J., de Leeuw, J.W., 2001. Temporal variations in C-13 and C-14
1022 concentrations in particulate organic matter from the southern North Sea. *Geochim.*
1023 *Cosmochim. Acta* 65, 2899-2911.

1024 Millot, C., 1990. The Gulf Of Lions Hydrodynamics. *Cont. Shelf Res.* 10, 885-894.

1025 Miralles, J., Radakovitch, O., Aloisi, J.C., 2005. Pb-210 sedimentation rates from the
1026 Northwestern Mediterranean margin. *Mar. Geol.* 216, 155-167.

1027 Mook, W.G., van der Plicht, J., 1999. Reporting C-14 activities and concentrations.
1028 *Radiocarbon* 41, 227-239.

1029 Nagao, S., Usui, T., Yamamoto, M., Minagawa, M., Iwatsuki, T., Noda, A., 2005. Combined
1030 use of delta C-14 and delta C-13 values to trace transportation and deposition processes of
1031 terrestrial particulate organic matter in coastal marine environments. *Chemical Geology* 218,
1032 63-72.

1033 Ollivier, P., Hamelin, B., Radakovitch, O., 2010. Seasonal variations of physical and chemical
1034 erosion: A three-year survey of the Rhone River (France). *Geochim. Cosmochim. Acta* 74,
1035 907-927.

1036 Opsahl, S., Benner, R., 1995. Early diagenesis of vascular plant tissues - Lignin and cutin
1037 decomposition and biogeochemical implications. *Geochim. Cosmochim. Acta* 59, 4889-4904.

1038 Panagiotopoulos, C., Sempere, R., Para, J., Raimbault, P., Rabouille, C., Charriere, B., 2012.
1039 The composition and flux of particulate and dissolved carbohydrates from the Rhone River
1040 into the Mediterranean Sea. *Biogeosciences* 9, 1827-1844.

1041 Pastor, L., Cathalot, C., Deflandre, B., Viollier, E., Soetaert, K., Meysman, F.J.R., Ulses, C.,
1042 Metzger, E., Rabouille, C., 2011a. Modeling biogeochemical processes in sediments from the
1043 Rhone River prodelta area (NW Mediterranean Sea). *Biogeosciences* 8, 1351-1366.

1044 Pastor, L., Deflandre, B., Viollier, E., Cathalot, C., Metzger, E., Rabouille, C., Escoubeyrou,
1045 K., Lloret, E., Pruski, A.M., Vétion, G., Desmalades, M., Buscail, R., Gremare, A., 2011b.
1046 Influence of the organic matter composition on benthic oxygen demand in the Rhone River
1047 prodelta (NW Mediterranean Sea). *Cont. Shelf Res.* 31, 1008-1019.

1048 Pont, D., Simonnet, J.P., Walter, A.V., 2002. Medium-term changes in suspended sediment
1049 delivery to the ocean: Consequences of catchment heterogeneity and river management
1050 (Rhone River, France). *Estuar. Coast. Shelf Sci.* 54, 1-18.

1051 Radakovitch, O., Charmasson, S., Arnaud, M., Bouisset, P., 1999a. Pb-210 and caesium
1052 accumulation in the Rhone delta sediments. *Estuar. Coast. Shelf Sci.* 48, 77-92.

1053 Radakovitch, O., Cherry, R.D., Heussner, S., 1999b. Pb-210 and Po-210: tracers of particle
1054 transfer on the Rhone continental margin (NW Mediterranean). *Deep-Sea Res. Part I-*
1055 *Oceanogr. Res. Pap.* 46, 1539-1563.

1056 Raymond, P.A., Bauer, J.E., 2001a. Riverine export of aged terrestrial organic matter to the
1057 North Atlantic Ocean. *Nature* 409, 497-500.

1058 Raymond, P.A., Bauer, J.E., 2001b. Use of C-14 and C-13 natural abundances for evaluating
1059 riverine, estuarine, and coastal DOC and POC sources and cycling: a review and synthesis.
1060 *Organic Geochemistry* 32, 469-485.

1061 Richy, P., 1992. Contribution à l'étude des mécanismes et bilans de l'érosion chimiques des „
1062 Terres Noires “ du bassin de la Durance. Exemple des bassins versants expérimentaux de la
1063 région de Draix (N-E de Digne). University of Aix-Marseille III, France, Marseille, p. 41.

1064 Roussiez, V., Aloisi, J.C., Monaco, A., Ludwig, W., 2005. Early muddy deposits along the
1065 Gulf of Lions shoreline: A key for a better understanding of land-to-sea transfer of sediments
1066 and associated pollutant fluxes. *Mar. Geol.* 222, 345-358.

1067 Roussiez, V., Ludwig, W., Monaco, A., Probst, J.L., Bouloubassi, I., Buscail, R., Saragoni,
1068 G., 2006. Sources and sinks of sediment-bound contaminants in the Gulf of Lions (NW
1069 Mediterranean Sea): A multi-tracer approach. *Cont. Shelf Res.* 26, 1843-1857.

1070 Salmon, V., Derenne, S., Lallier-Verges, E., Largeau, C., Beaudoin, B., 2000. Protection of
1071 organic matter by mineral matrix in a Cenomanian black shale. *Organic Geochemistry* 31,
1072 463-474.

1073 Sempéré, R., Charriere, B., Van Wambeke, F., Cauwet, G., 2000. Carbon inputs of the Rhone
1074 River to the Mediterranean Sea: Biogeochemical implications. *Glob. Biogeochem. Cycle* 14,
1075 669-681.

1076 Sheesley, R.J., Krusa, M., Krecl, P., Johansson, C., Gustafsson, O., 2009. Source
1077 apportionment of elevated wintertime PAHs by compound-specific radiocarbon analysis.
1078 *Atmospheric Chemistry and Physics* 9, 3347-3356.

1079 Siani, G., Paterne, M., Michel, E., Sulpizio, R., Sbrana, A., Arnold, M., Haddad, G., 2001.
1080 Mediterranean Sea surface radiocarbon reservoir age changes since the last glacial maximum.
1081 *Science* 294, 1917-1920.

1082 Stuiver, M., Polach, H.A., 1977. Reporting of ^{14}C data - Discussion. *Radiocarbon* 19, 355-
1083 363.

1084 Tauler, R., Kowalski, B., Fleming, S., 1993. Multivariate curve resolution applied to spectral
1085 data from multiple runs of an industrial-process. *Analytical Chemistry* 65, 2040-2047.

1086 Tesi, T., Goñi, M.A., Langone, L., Puig, P., Canals, M., Nittrouer, C.A., Durrieu de Madron,
1087 X., Calafat, A., Palanques, A., Heussner, S., Davies, M.H., Drexler, T.M., Fabres, J.,
1088 Miserocchi, S., 2010a. Reexposure and advection of ^{14}C -depleted organic carbon from old
1089 deposits at the upper continental slope. *Global Biogeochem. Cycles* 24, GB4002.

1090 Tesi, T., Miserocchi, S., Goni, M.A., Langone, L., 2007a. Source, transport and fate of
1091 terrestrial organic carbon on the western Mediterranean Sea, Gulf of Lions, France. *Mar.*
1092 *Chem.* 105, 101-117.

1093 Tesi, T., Miserocchi, S., Goni, M.A., Langone, L., Boldrin, A., Turchetto, M., 2007b. Organic
1094 matter origin and distribution in suspended particulate materials and surficial sediments from
1095 the western Adriatic Sea (Italy). *Estuar. Coast. Shelf Sci.* 73, 431-446.

1096 Tesi, T., Puig, P., Palanques, A., Goni, M.A., 2010b. Lateral advection of organic matter in
1097 cascading-dominated submarine canyons. *Progress in Oceanography* 84, 185-203.

1098 Tolosa, I., Bayona, J.M., Albaiges, J., 1996. Aliphatic and polycyclic aromatic hydrocarbons
1099 and sulfur/oxygen derivatives in northwestern Mediterranean sediments: Spatial and temporal
1100 variability, fluxes, and budgets. *Environmental Science & Technology* 30, 2495-2503.

1101 Toussaint, F., Tisnérat-Laborde, N., Cathalot, C., Buscail, R., Kerhervé, P., Rabouille, C.,
1102 accepted. Depositional processes of organic matter in the Rhône River Delta (Gulf of Lions,
1103 France) traced by density fractionation coupled with $\Delta^{14}\text{C}$ and $\delta^{13}\text{C}$. Radiocarbon.
1104 Tronczynski, J., Munsch, C., Heas-Moisan, K., Guiot, N., Truquet, I., Olivier, N., Men, S.,
1105 Furaut, A., 2004. Contamination of the Bay of Biscay by polycyclic aromatic hydrocarbons
1106 (PAHs) following the T/V "Erika" oil spill. Aquatic Living Resources 17, 243-259.
1107 Ulses, C., Estournel, C., de Madron, X.D., Palanques, A., 2008. Suspended sediment transport
1108 in the Gulf of Lions (NW Mediterranean): Impact of extreme storms and floods. Cont. Shelf
1109 Res. 28, 2048-2070.
1110 Wakeham, S.G., Canuel, E.A., Lerberg, E.J., Mason, P., Sampere, T.P., Bianchi, T.S., 2009.
1111 Partitioning of organic matter in continental margin sediments among density fractions. Mar.
1112 Chem. 115, 211-225.
1113 Wang, X.C., Druffel, E.R.M., Griffin, S., Lee, C., Kashgarian, M., 1998. Radiocarbon studies
1114 of organic compound classes in plankton and sediment of the northeastern Pacific Ocean.
1115 Geochim. Cosmochim. Acta 62, 1365-1378.
1116 White, H.K., Reddy, C.M., Eglinton, T.I., 2008. Radiocarbon-based assessment of fossil fuel-
1117 derived contaminant associations in sediments. Environmental Science & Technology 42,
1118 5428-5434.
1119 White, H.K., Reddy, C.M., Eglinton, T.I., 2005. Isotopic constraints on the fate of petroleum
1120 residues sequestered in salt marsh sediments. Environmental Science & Technology 39, 2545-
1121 2551.
1122 Williams, P.M., Robertson, K.J., Soutar, A., Griffin, S.M., Druffel, E.R.M., 1992. Isotopic
1123 Signatures (C-14 , C-13 , N-15) As Tracers Of Sources And Cycling Of Soluble And
1124 Particulate Organic-Matter In The Santa-Monica Basin, California. Progress In Oceanography
1125 30, 253-290.

1126 Wright, L.D., Friedrichs, C.T., 2006. Gravity-driven sediment transport on continental
1127 shelves: A status report. *Cont. Shelf Res.* 26, 2092-2107.

1128 Yechieli, Y., Sivan, O., Lazar, B., Vengosh, A., Ronen, D., Herut, B., 2001. Radiocarbon in
1129 seawater intruding into the Israeli Mediterranean coastal aquifer. *Radiocarbon* 43, 773-781.

1130 Yunker, M.B., Perreault, A., Lowe, C.J., 2012. Source apportionment of elevated PAH
1131 concentrations in sediments near deep marine outfalls in Esquimalt and Victoria, BC, Canada:
1132 Is coal from an 1891 shipwreck the source? *Organic Geochemistry* 46, 12-37.

1133 Zonneveld, K.A.F., Versteegh, G.J.M., Kasten, S., Eglinton, T.I., Emeis, K.C., Huguet, C.,
1134 Koch, B.P., de Lange, G.J., de Leeuw, J.W., Middelburg, J.J., Mollenhauer, G., Prahl, F.G.,
1135 Rethemeyer, J., Wakeham, S.G., 2010. Selective preservation of organic matter in marine
1136 environments; processes and impact on the sedimentary record. *Biogeosciences* 7, 483-511.

1137 Zuo, Z., Eisma, D., Gieles, R., Beks, J., 1997. Accumulation rates and sediment deposition in
1138 the northwestern Mediterranean. *Deep-Sea Research Part Ii-Topical Studies In Oceanography*
1139 44, 597-609.

1140

1141

1142

1143

1144

1145 Table 1. Summary of intermediate and bottom waters conditions in April 2007 cruise. Distance
 1146 is reported respective to the Rhône River mouth.
 1147

	Stations	Lat. (°N)	Long. (°E)	Distance (km)	Depth (m)	T (°C)	SPM mg l ⁻¹	[POC] (µgC l ⁻¹)	[POC] (%)	δ ¹³ C (‰)	Δ ¹⁴ C (‰)		Radiocarbon ages (yr)	
Prodelta area	A	43° 18' 48"	4° 51' 6"	1.9	13	14.9	1.6	152.3	9.3	-23.4	29.2	+ 0.2	post-bomb	
					25	15.2	2.8	217.6	7.8	-24.1	-72.8	+ 0.1	609 :87	
	B	43° 18' 11"	4° 50' 8"	3.1	25	14.8	2.1	247.6	11.9	-21.7	-168.0	+ 0.1	1479.0 :86	
					57	14.8	5.0	207.6	4.2	-24.4	-212.8	+ 0.1	1930 :110	
	K	43° 18' 7"	4° 51' 28"	3.3	31	15.3	0.9	106.5	11.4	-24.1	-	-	-	
					63	14.8	2.9	137.2	4.8	-23.5	-	-	-	
	L	43° 18' 6"	4° 52' 48"	4.2	66	14.3	2.0	218.4	11.0	-	-	-	-	
Continental shelf	C	43° 16' 21"	4° 46' 44"	8.3	40	14.8	1.9	-	-	-	-	-	-	
					76	14.5	4.1	159.2	3.9	-23.8	-298.2	+ 0.1	2847 :98	
	D	43° 15' 3"	4° 43' 48"	12.8	73	14.3	2.8	152.2	5.5	-23.7	-	-	-	
	E	43° 13' 18"	4° 41' 59"	16.8	35	14.5	1.8	117.0	6.4	-23.2	-67.8	+ 0.1	561 :86	
					75	14.2	3.5	146.0	4.2	-24.4	-320.4	+ 0.1	3106 :92	
	F	43° 10' 10"	4° 39' 1"	23.8	40	14.4	1.6	120.2	7.4	-23.9	-	-	-	
					78	14.2	3.1	155.5	5.0	-24.1	-	-	-	
	G	43° 18' 30"	4° 47' 17"	5.2	47	14.8	5.0	174.3	3.5	-	-	-	-	
	H	43° 15' 54"	4° 49' 11"	7.5	40	15.1	1.3	105.5	8.3	-23.1	-	-	-	
					86	14.5	2.3	137.3	6.1					
	I	43° 15' 59"	4° 53' 0"	7.7	89	15.1	5.4	181.4	3.4	-23.8	-	-	-	
J	43° 18' 15"	4° 58' 2"	10.3	86	14.1	1.3	105.1	7.9	-24.3	-111.8	+ 0.1	958 :92		
M	43° 9' 59"	4° 44' 4"	20.3	91	14.1	2.1	137.3	6.7	-	-	-	-		
N	43° 17' 29"	4° 48' 3"	5.6	3	15.2	2.4	265.7	11.0	-23.0	-	-	-		
				32	15.2	2.4	123.9	5.2	-23.2	-	-	-		
				67	14.5	5.2	-	-	-	-	-	-		
O	43° 16' 58"	4° 49' 44"	5.4	79	14.4	2.8	137.3	4.8	-24.4	-	-	-		
R2	43° 14' 28"	4° 52' 55"	10.3	98	14.1	0.8	77.4	9.7	-23.8	-	-	-		
Rhône									1.6	-27.1	147.7	+ 2.8	post-bomb	
									1.9	-27.5	77.8	+ 2.8	post-bomb	
									0.8★	-25.8★	-495.1★	+ 1.7	5510 :30	
									1.6	-27.2	40.6	+ 3.1	post-bomb	
													;	
										2.7	-26.8	-89.7	+ 2.6	757 :25
													;	
									1.6	-27.8	-37.0	+ 2.8	304 :24	

1148
 1149 ★ indicate the June 2008 atypical flood originating from the Durance basin.
 1150

1151 Table 2. Isotopic OC parameters from selected stations of the Rhône prodelta sediments

1152

	Stations	Lat. (°N)	Long. (°E)	Depth (m)	Distance (km)	Cruise	Sediment depth (cm)	C _{org} (%)	δ ¹³ C (‰)	Δ14C (‰)	Age ¹⁴ Coc (yr BP)	Λ _s Syringyl + Vanyllin Phenols*	δ ¹³ C _{SV} (‰) Syringinc + Vanillin pool
Prodelta transition area	A	43° 18' 47"	4° 51' 4"	24	1.93	Jun-05	0-1	1.81	-26.8	143 ± -14	modern	3.18 ± 0.07	-31.3
							3-4	1.92	-27.1	128 ± -14	modern	3.16 ± 0.27	-30.3
							Apr-07	0-1	1.99	-27.2	59 ± -2	modern	-
	B	43° 18' 14"	4° 50' 4"	54	3.02	Jun-05	0-1	1.68	-26.7	13 ± -14	modern	-	-
							3-4	1.55	-26.7	53 ± -13	modern	-	-
							Apr-07	0-1	1.61	-26.6	7 ± -3	modern	-
	K	43° 18' 7"	4° 51' 29"	62	3.28	Jun-05	0-1	1.18	-26.2	-8 ± -14	65	-	-
							3-4	1.10	-26.2	-80 ± -13	675	-	-
							Apr-07	0-1	1.79	-26.7	-	-	-
	L	43° 18' 24"	4° 52' 59"	62	4.03	Jun-05	0-1	1.15	-25.9	-121 ± -10	1035	-	-
							3-4	1.28	-26.0	-102 ± -10	865	-	-
							Apr-07	0-1	1.51	-26.3	-	-	-
Continental shelf	C	43° 16' 17"	4° 46' 33"	76	8.57	Jun-05	0-1	1.02	-25.3	-218 ± -9	1980	1.76 ± 0.07	-28.1
							3-4	1.03	-25.3	-222 ± -8	2025	1.49 ± 0.14	-29.7
							Apr-07	0-1	1.25	-25.4	-226 ± -2	2075	-
	D	43° 14' 54"	4° 43' 46"	74	13.01	Jun-05	0-1	0.93	-24.5	-263 ± -8	2450	-	-
							3-4	0.93	-24.7	-255 ± -8	2365	-	-
							Apr-07	0-1	1.05	-24.8	-	-	-
	E	43° 13' 12"	4° 41' 54"	75	17.03	Jun-05	0-1	0.89	-24.3	-312 ± -7	3010	0.32 ± 0.06	-27
							3-4	0.90	-24.3	-319 ± -7	3095	0.31 ± -	-23
							Apr-07	0-1	-	-24.5	-	-	-
	F	43° 10' 1"	4° 41' 59"	78	21.61	Jun-05	0-1	-	-	-	-	-	-
							3-4	-	-	-	-	-	-
							Apr-07	0-1	1.43	-24.2	-400 ± -4	4120	-
	H	43° 15' 53"	4° 49' 10"	86	7.52	Jun-05	0-1	1.03	-25.2	-217 ± -8	1965	-	-
							3-4	1.03	-25.5	-249 ± -7	2305	-	-
							Apr-07	0-1	1.17	-25.6	-	-	-
	I	43° 16' 0"	4° 53' 1"	89	7.68	Jun-05	0-1	0.82	-24.3	-115 ± -11	980	-	-
							3-4	0.88	-24.5	-330 ± -7	3215	-	-
							Apr-07	0-1	1.03	-25.1	-	-	-
	J	43° 16' 7"	4° 58' 6"	86	12.09	Jun-05	0-1	0.82	-23.9	-386 ± -6	3925	-	-
							3-4	0.97	-24.1	-393 ± -6	4010	-	-
							Apr-07	0-1	-	-	-	-	-
	N	43° 17' 33"	4° 47' 59"	67	5.54	Jun-05	0-1	-	-	-	-	-	-
							3-4	-	-	-	-	-	-
							Apr-07	0-1	1.43	-25.9	-	-	-
O	43° 17' 0"	4° 50' 6"	79	5.22	Jun-05	0-1	-	-	-	-	-	-	
						3-4	-	-	-	-	-	-	
						Apr-07	0-1	1.43	-25.7	-	-	-	-
H30	43° 18' 42"	4° 49' 34"	30	2.55		0-1	1.67	-27	-199		2.7 ⁺	-	
SO66	43° 18' 32"	4° 30' 31"	67	29.59		0-1	0.89	-23.9	-358		0.6 ⁺	-	
SK63	43° 20' 4"	4° 6' 19"	65	59.82		0-1	0.81	-23.3	-412			-	
SC63	43° 0' 31"	3° 19' 21"	64	128.54		0-1	0.83	-22.9	-399			-	

1153

1154 The error in AgeOC is ± 30 years for all samples.

1155 * Units: mg/100mgOC. Sum of vanillyl + syringyl phenol yields (Λ_6) was calculated by
1156 excluding cinnamyl phenols to compare directly to previous data (Sheesley et al, 2009)

1157 † Sum of vanillyl + syringyl + cinnamyl phenol yields (Λ_8) (Tesi et al, 2007)

1158

1159 Table 3: Composition of lignin parameters obtained in April 2007 from selected stations of the Rhône prodelta and adjacent continental shelf
 1160 sediments

Stations	Sediment depth (cm)	S*	V*	C*	P*		PON/P		S/V		C/V		(Ad/Al) _v		P/(S+V)	
		<i>Syringyl Phenols</i>	<i>Vanillin Phenols</i>	<i>Cinnamyl Phenols</i>	<i>p-hydroxyl Phenols</i>		<i>PON/p-hydroxyl ratio</i>	<i>Syringyl/Vanillin ratio</i>	<i>Cinnamyl/Vanillin ratio</i>	<i>Vanillin acid/aldehyde ratio</i>						
A	1-2	1.40 ± 0.10	1.77 ± 0.03	0.20 ± 0.03	2.13 ± 0.05	0.042 ± 0.018	0.79 ± 0.07	0.11 ± 0.02	0.32 ± 0.04	0.67 ± 0.04						
	3-4	1.41 ± 0.25	1.75 ± 0.01	0.23 ± 0.00	1.63 ± 0.18	0.049 ± 0.000	0.81 ± 0.14	0.13 ± 0.00	0.31 ± 0.05	0.52 ± 0.12						
C	1-2	0.45 ± 0.09	1.31 ± 0.02	0.23 ± 0.05	1.87 ± 0.14	0.031 ± 0.018	0.35 ± 0.07	0.18 ± 0.03	0.43 ± 0.05	1.06 ± 0.15						
	3-4	0.48 ± 0.07	1.01 ± 0.06	0.12 ± 0.06	1.52 ± 0.07	0.027 ± 0.003	0.47 ± 0.05	0.12 ± 0.06	0.28 ± 0.33	1.02 ± 0.03						
E	1-2	0.09 ± 0.02	0.23 ± 0.03	0.02 ± 0.01	0.38 ± 0.02	0.037 ± 0.004	0.40 ± 0.04	0.07 ± 0.03	0.37 ± 0.12	1.17 ± 0.10						
	3-4	0.08 ± -	0.23 ± -	0.02 ± -	0.31 ± -	0.048 ± -	0.36 ± -	0.08 ± -	0.29 ± -	1.00 ± -						

		$\delta^{13}C_{S,V}$ (‰)	$\delta^{13}C_{SI}$ (‰)	$\delta^{13}C_{Sd}$ (‰)	$\delta^{13}C_{Sn}$ (‰)	$\delta^{13}C_{VI}$ (‰)	$\delta^{13}C_{Vn}$ (‰)	$\delta^{13}C_{Vd}$ (‰)	$\delta^{13}C_{pC}$ (‰)
		<i>Syringinc+Vanillin pool</i>	<i>Syringaldehyde</i>	<i>Syringic Acid</i>	<i>Acetosyringone</i>	<i>Vanillin</i>	<i>Acetovanillone</i>	<i>Vanillic Acid</i>	<i>p-Coumaric Acid</i>
A	1-2	-31.3 ± 0.5	-28.7 ± 1.8	-39.9 ± 1.4	-31.3 ± 0.8	-29.9 ± 0.3	-29.1 ± 0.8	-38.7 ± 0.5	-32.8
	3-4	-30.3 ± 0.3	-30.4 ± 0.4	-34.4 ± 1.7	-30.1 ± 0.6	-28.5 ± 0.7	-28.2 ± 0.6	-35.6 ± 0.8	-30.8
C	1-2	-28.1 ± 0.5	-24.1 ± -	-32.5 ± 2.3	-32.8 ± 1.6	-26.2 ± 0.1	-29.0 ± 3.6	-32.2 ± 1.3	
	3-4	-29.7 ± 0.8	-27.5 ± 2.5	-29.2 ± 0.2	-33.2 ± 2.1	-28.7 ± 1.1	-28.3 ± 2.8	-36.8 ± 1.3	
E	1-2	-27.0 ± 0.8	-21.9 ± -	-29.1 ± 2.9	-24.5 ± 2.5	-27.9 ± 1.3	-32.1 ± 4.2	-27.0 ± 0.7	
	3-4	-23.0 ± 1.4	-13.9 ± 5.6	-30.1 ± -	-30.9 ± 3.7	-18.0 ± 2.0	-28.7 ± 0.6	-39.6 ± 3.8	

1162

1163

1164 * units: mg/100mgOC

1165 Sum of vanillyl + syringyl phenol yields (Λ_6) was calculated by excluding cinnamyl phenols to compare directly to previous data (Tesi et al,
1166 2007).

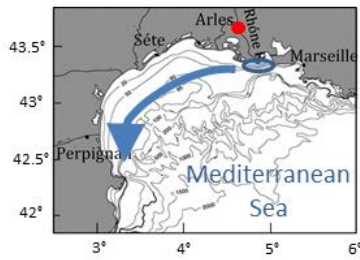
1167 Several compounds were used as internal standards for lignin oxidation, extraction, and analysis. Based off ethyl vanillin, the precision is
1168 $\pm 0.84\%$. It is greater for the other internal standards: 3.50% for cinnamic acid, and 1.77% for 3,4-dihydroxybenzoic acid. Ethyl vanillin and
1169 cinnamic acid both experience the full extraction method and derivitization, whereas 3,4-dihydroxybenzoic acid only experiences derivitization.
1170 Hence, 3,4-dihydroxybenzoic acid is most likely to be the most representative of instrumental variability

Table 4. PAH concentrations ($\mu\text{g}/\text{kg}$ d.w.) in the Rhône delta sediments.

Station	A	C	RHO 0*	RHO 1*
Lat. N	43°18.829N	43°16.286N	43°13.903N	43°13.903N
Long. E	04°51.145E	04°46.474E	04°50.457E	04°50.457E
Depth (m)	20	75	98	98
Sampling date	2005	2005	2008	2008
Layer (cm)	1-2	1-2	0-1	1-2
% OC (dw)	1.81	1.02	0.72	0.72
PAH total ($\mu\text{g}/\text{kg}$ d.w.)	2026.0	2074.0	2278.7	2360.4
ΣPAH_6 ($\mu\text{g}/\text{kg}$ d.w.)	501.0	447.3	554.0	598.2
PAH (parent; $\mu\text{g}/\text{kg}$ d.w.)	935.4	878.3	1055.1	1133.2
Petrogenic component (%)	28.6	31.6	30.1	29.3

* Continental shelf surface sediments - Rhosos cruise 2008, station KS30.

ΣPAH_6 is the summed concentrations of six indicator compounds: fluoranthene, benzo[*b*]fluoranthene, benzo[*k*]fluoranthene, benzo[*a*]pyrene, benzo[*ghi*]perlyene and indeno[123-*cd*]pyrene.



● Monitoring station

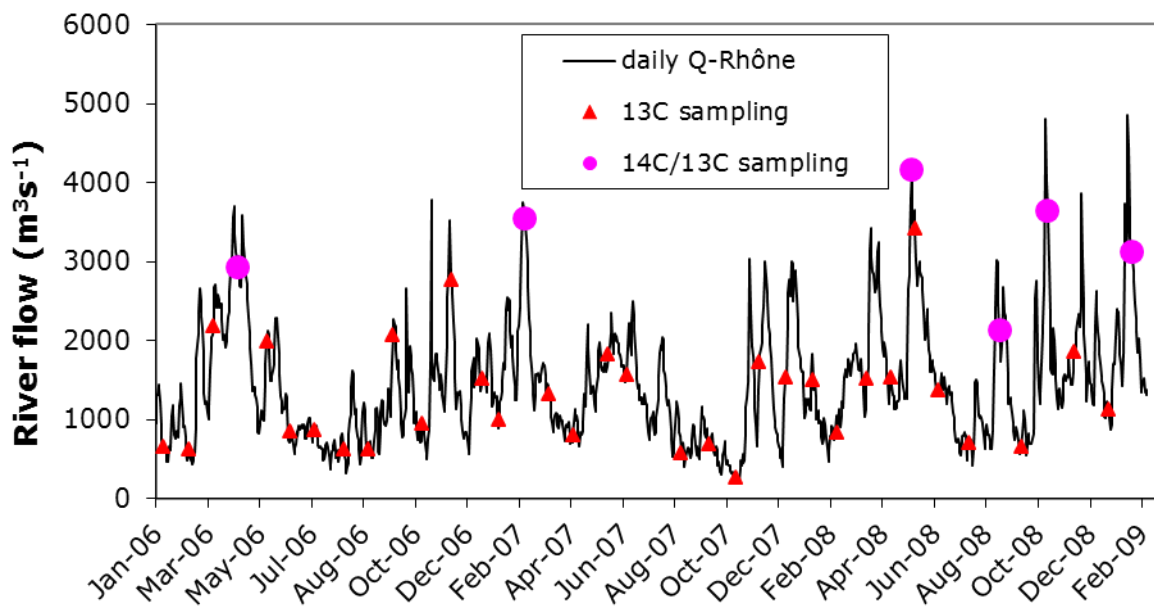
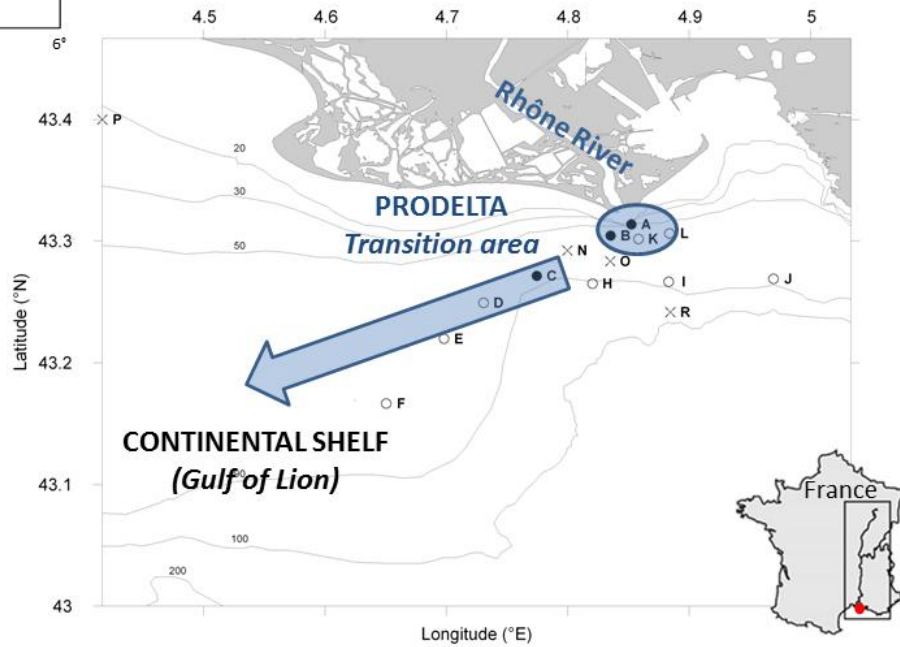


Figure 1.

Top panel. Map of the Rhône River prodelta indicating the locations of sampling stations, the main deposit entities and the main circulation direction. Circles indicate sampling stations for $\delta^{13}\text{C}$ and $\Delta^{14}\text{C}$ ($\delta^{13}\text{C}$ measured during both cruises). Filled symbols indicate that stations were sampled for $\Delta^{14}\text{C}$ at both cruises. Crosses indicate stations sampled only for $\delta^{13}\text{C}$ and just once (April 2007 cruise). The arrow represents the main dispersal system direction.

Bottom panel. Rhône River discharge rates between 2006 and 2009. Sampling points for $\delta^{13}\text{C}_{\text{POC}}$ (triangles) and $\Delta^{14}\text{C}_{\text{POC}}$ (diamond) in riverine SPM (Arles monitoring station) are also indicated.

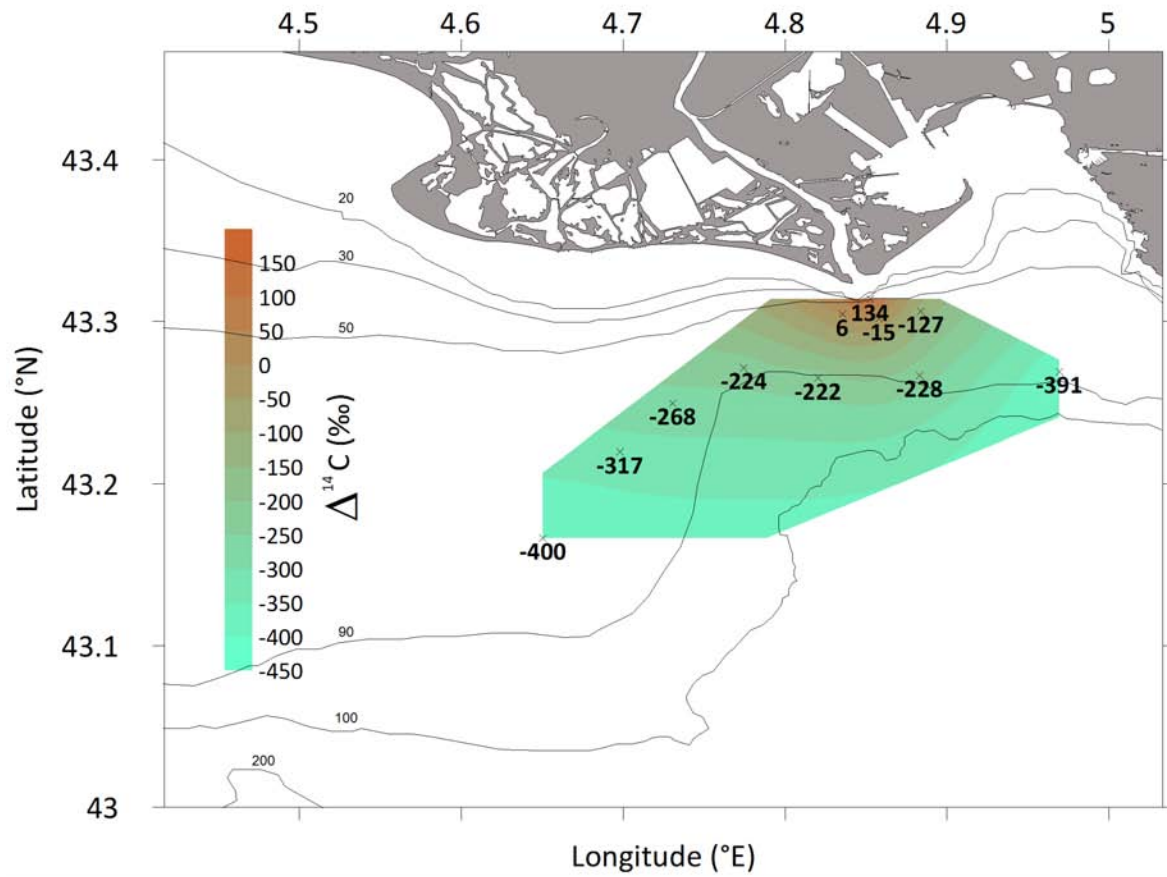


Figure 2. Spatial distribution of $\Delta^{14}\text{C}_{\text{OC}}$ in the Rhône River prodelta. Values close to 150 ‰ correspond to terrestrial enriched material whereas -400 ‰ indicates continental shelf old material.

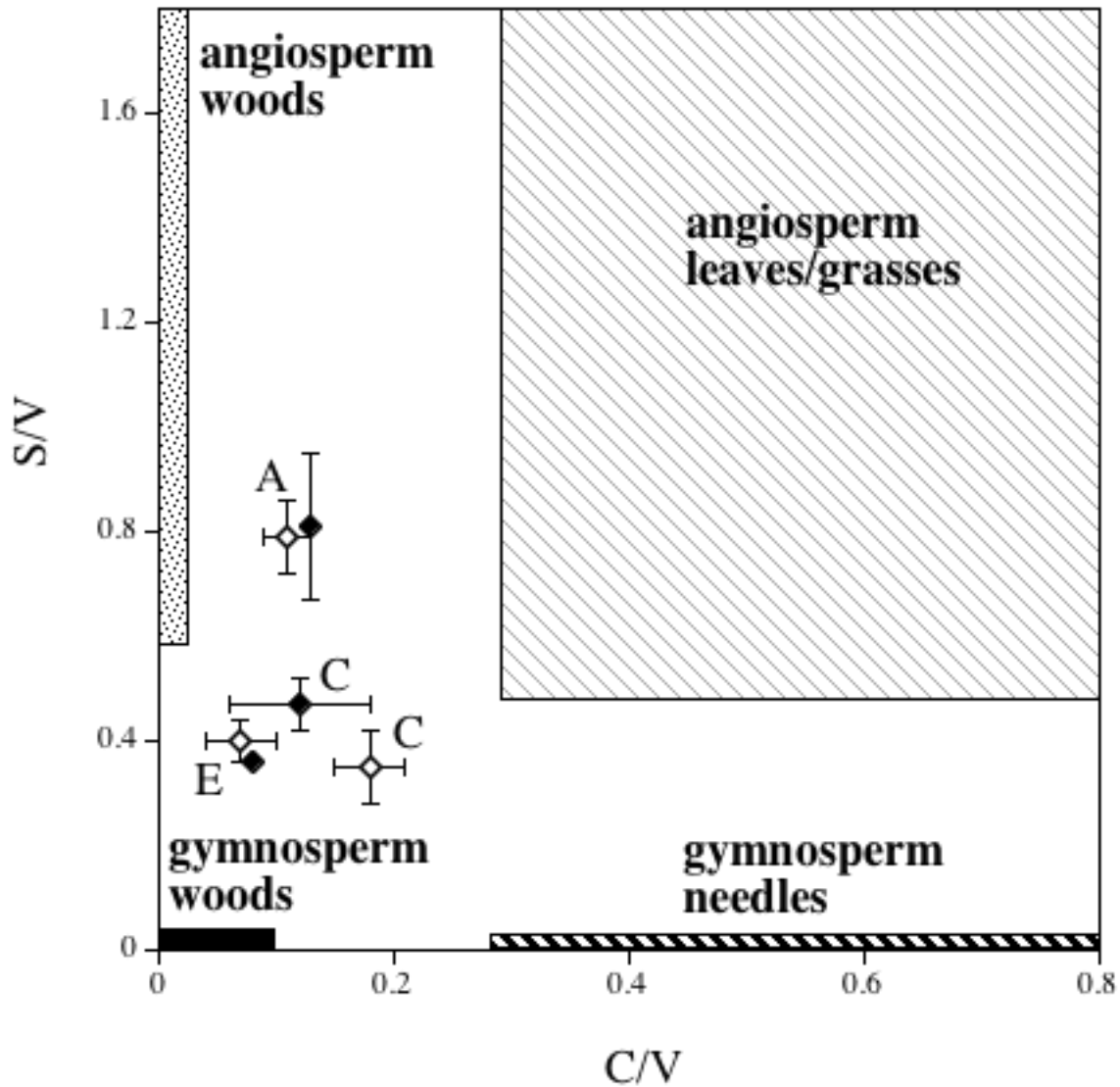
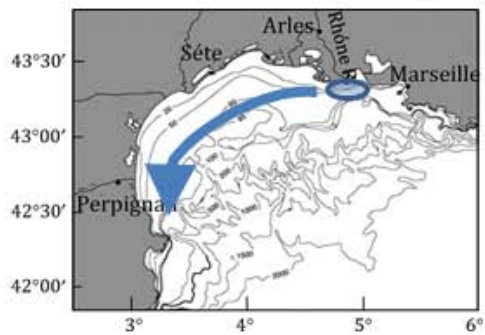


Figure 3. Plot of cinnamyl:vanillyl (C/V) vs. syringyl:vanillyl (S/V) phenol ratios for Rhône River sediments. Typical ranges for angiosperm and gymnosperm woody and non-woody tissue are indicated (Hedges and Mann, 1979; Goñi and Hedges, 1992). Open symbols represent the 1-2 cm sediment layer, and the filled symbols represent the 3-4 cm sediment layer. Stations are denoted by letter.



- this study
- Tesi et al (2007; 2010a,b)

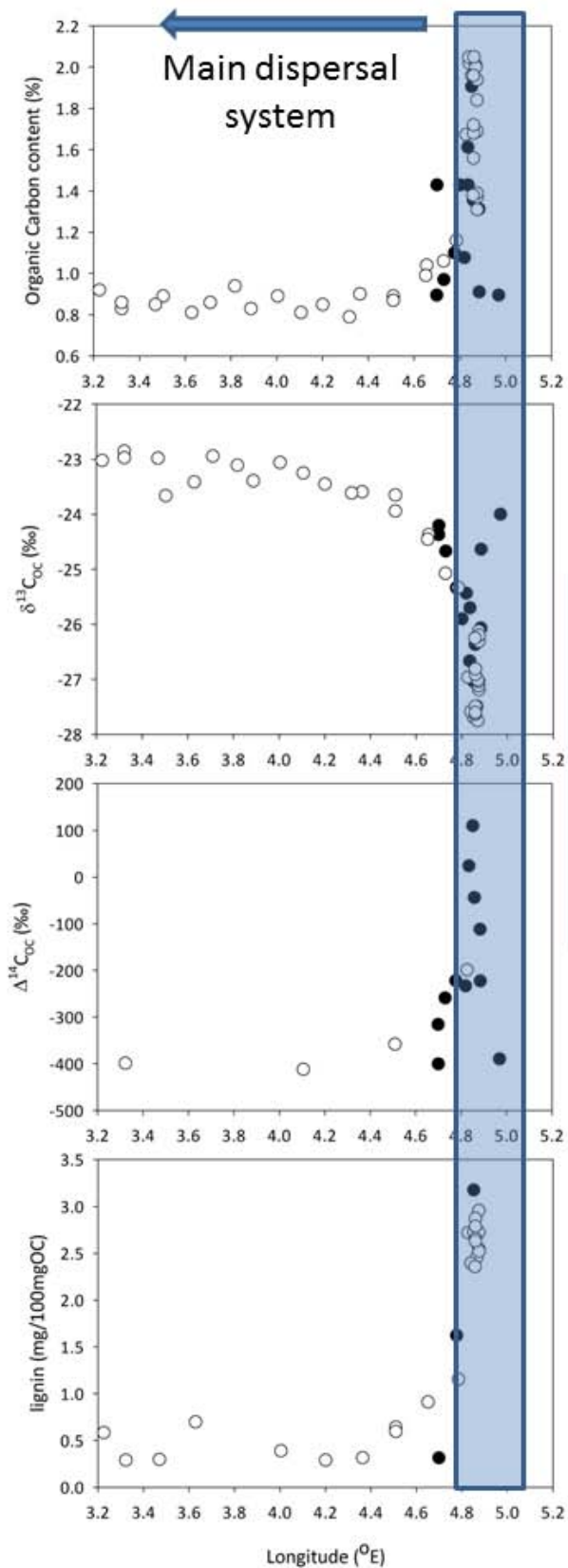


Figure 4. Biogeochemical parameters for surface sediment along the main dispersal system. The prodelta is highlighted as a transition zone for main biogeochemical characteristics. The continental shelf displays homogeneous values.

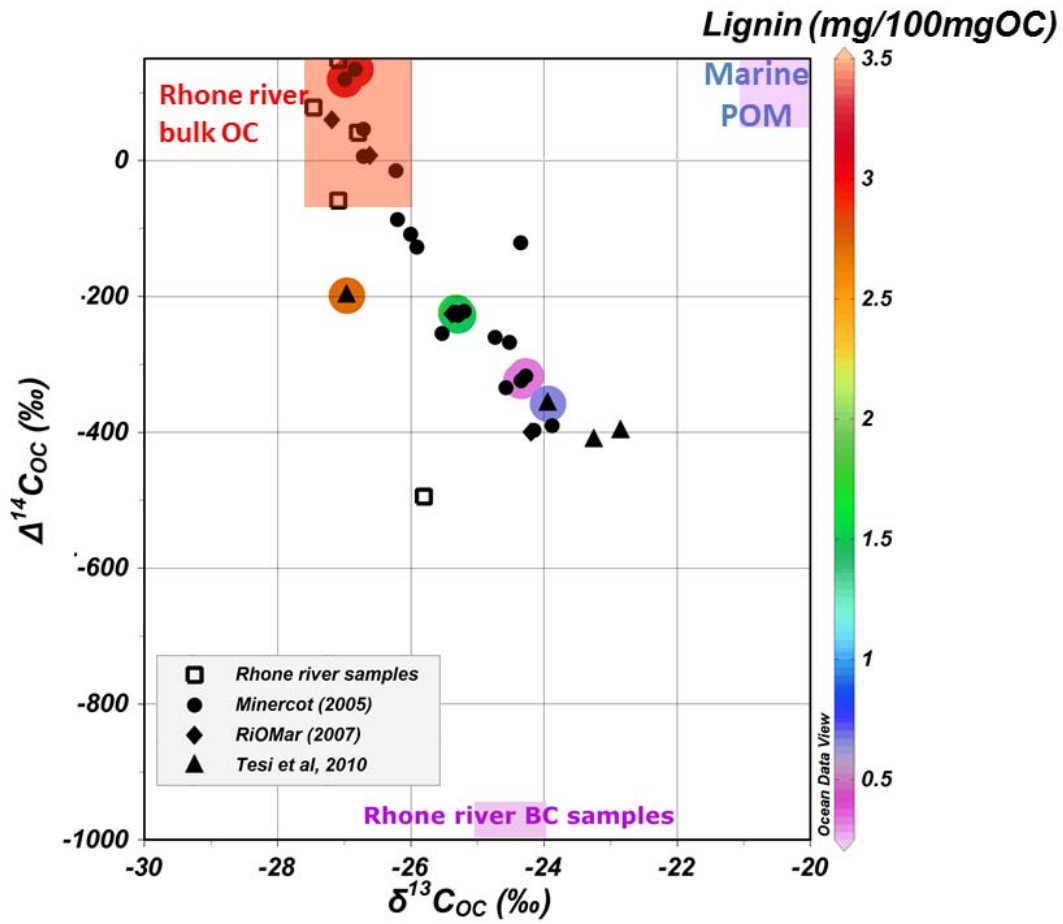


Figure 5. $\delta^{13}C_{OC}$ - $\Delta^{14}C_{OC}$ mixing plot with the Rhône River end-members (bulk and black carbon (BC)) plotted.

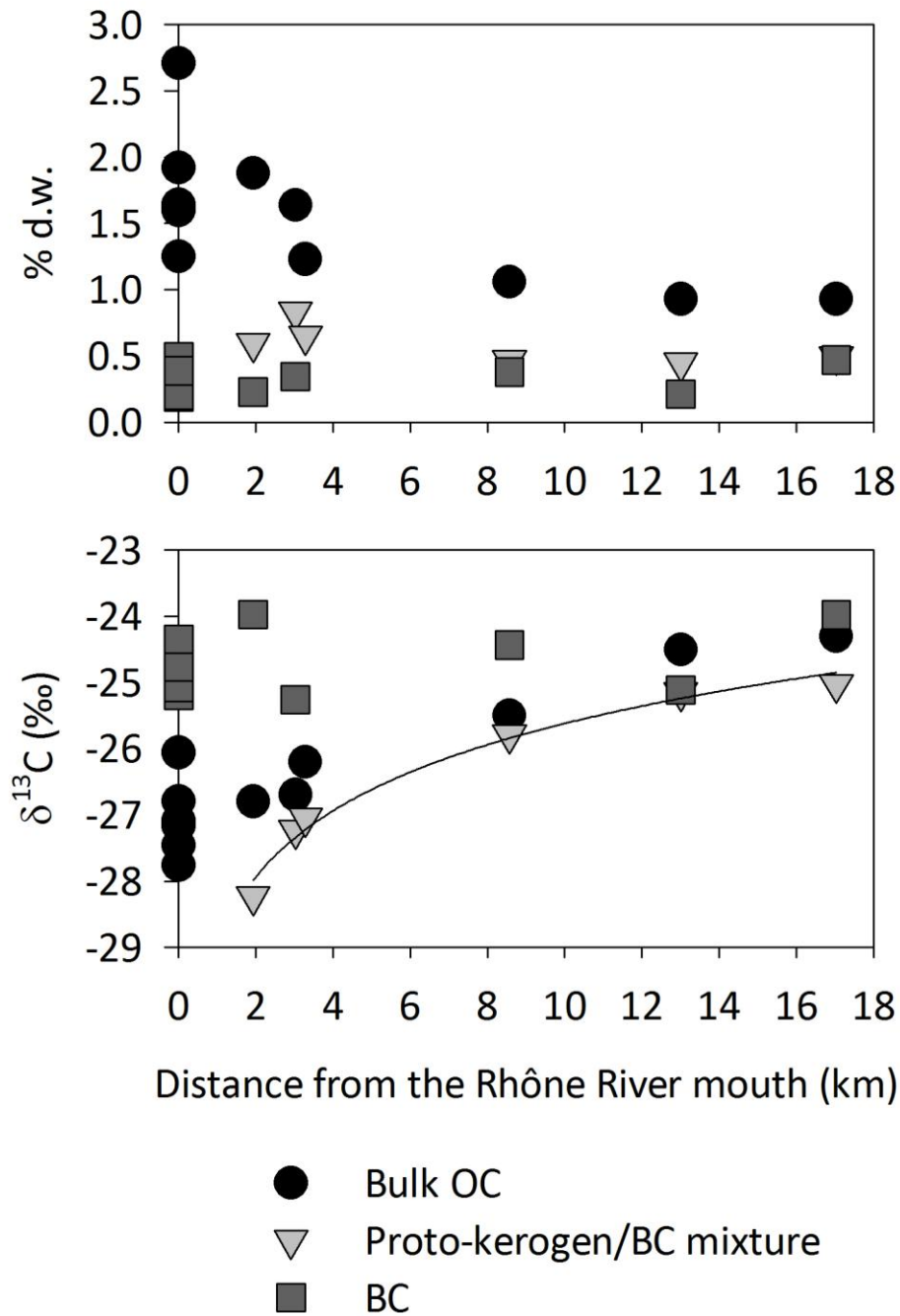


Figure 6. Bulk organic carbon (OC), black carbon (BC) and proto-kerogen/BC mixture contents (top) and respective $\delta^{13}\text{C}_{\text{OC}}$ signatures (bottom) in the Rhône River Suspended Particulate Matter and in the prodelta sediment. The regression line in the bottom panel indicate the trend for the proto-kerogen/BC mixture in the sediment as a function of distance with the river mouth.

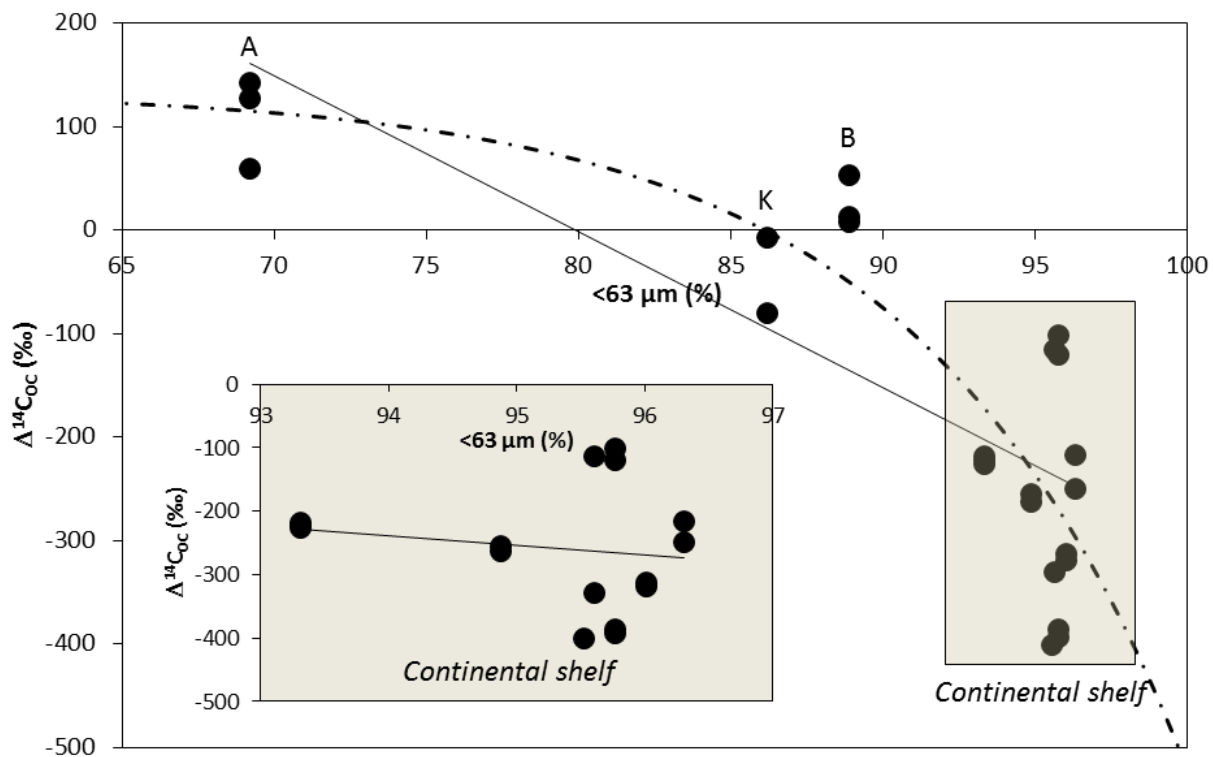


Figure 7. $\Delta^{14}\text{C}_{\text{OC}}$ - sand content correlation (%). The dashed line represents the exponential decay fit to the data. Stations A, B and K from the prodelta are indicated. Plain line figures the linear regression.

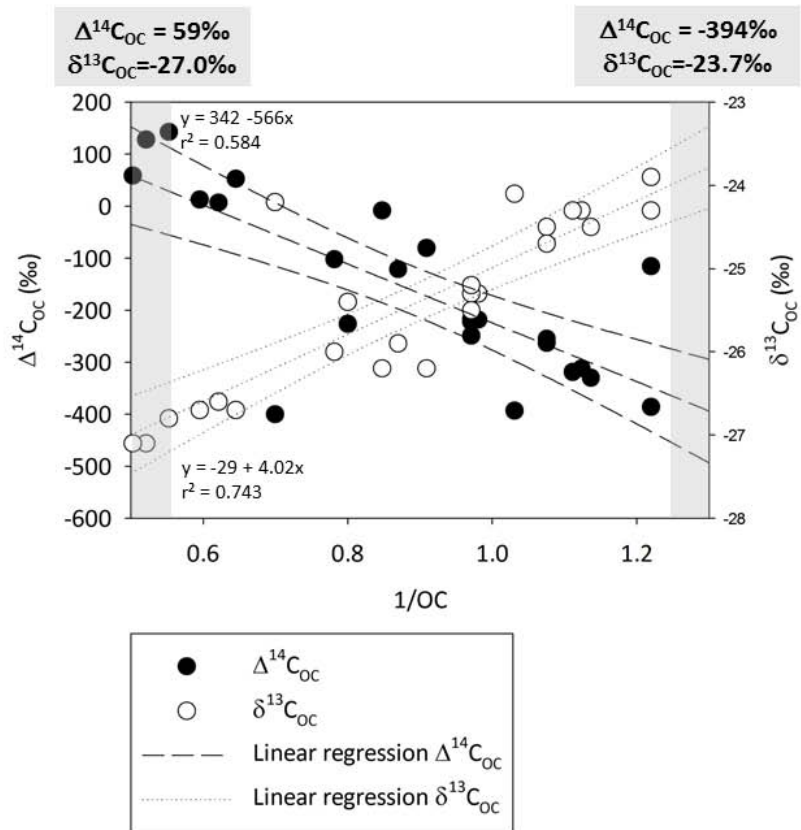


Figure 8. Mixing model of $\Delta^{14}\text{C}_{\text{OC}}$ (●) and $\delta^{13}\text{C}_{\text{OC}}$ (○) vs. $1/\text{OC}$. Net loss of terrestrial modern material as OC decrease in the system is indicated by the linear regression lines (dashed – dot for $\Delta^{14}\text{C}_{\text{OC}}$, and short dashed for $\delta^{13}\text{C}_{\text{OC}}$). Both the linear regression fit and its 95% confidence interval are represented.

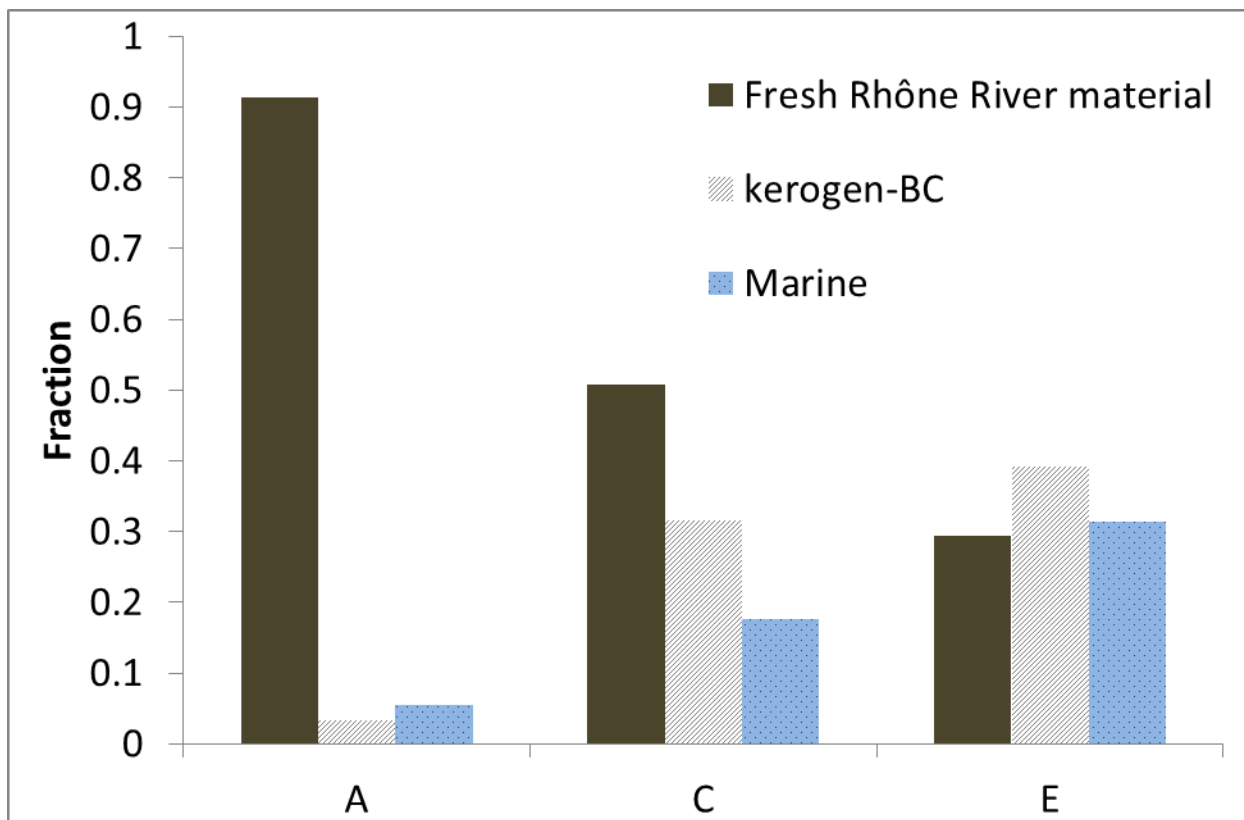


Fig. 9. Results of the mixing model considering 3 end-members: fresh terrestrial material from the Rhône River, a freshly produced marine phytoplankton (referred as marine) and a terrestrial mixture of kerogen-BC material (referred as kerogen-BC). Contributions are reported as fraction of OC.